Copy 336
RM L54F08

NACA RM L54F08

NACA

RESEARCH MEMORANDUM

PRESSURE DISTRIBUTIONS ON PLUG- AND SEMAPHORE-TYPE SPOILER AILERONS ON A 35° SWEPTBACK WING OF ASPECT RATIO 4, TAPER RATIO 0.6, AND NACA 65A006 AIRFOIL SECTION AT HIGH SUBSONIC SPEEDS

By Alexander D. Hammond and William C. Hayes, Jr.

Langley Aeronautical Laboratory
Langley Field, Va.

CLASSIFIED DOCUMENT

NATIONAL ADVISORY COMMITTEE FOR AERONAUTICS

WASHINGTON

August 30, 1954

NATIONAL ADVISORY COMMITTEE FOR AERONAUTICS

RESEARCH MEMORANDUM

PRESSURE DISTRIBUTIONS ON PLUG- AND SEMAPHORE-TYPE SPOILER AILERONS ON A 35° SWEPTBACK WING OF ASPECT RATIO 4, TAPER RATIO 0.6, AND NACA 65A006 AIRFOIL SECTION AT HIGH SUBSONIC SPEEDS

By Alexander D. Hammond and William C. Hayes, Jr.

SUMMARY

An investigation was made in the Langley high-speed 7- by 10-foot tunnel to determine the pressure distribution at the 20-, 46-, and 65-percent wing semispan stations on a plug-type spoiler extending from 14 to 98 percent of the wing semispan and on one segment of a semaphore-type spoiler extending from 13 to 33 percent of the wing semispan. The spoilers were located along the 70-percent chord line of a steel semispan wing which had a quarter-chord sweepback of 35°, an aspect ratio of 4, a taper ratio of 0.6, and NACA 65A006 airfoil sections parallel to free stream. The investigation was made through a Mach number range from 0.60 to 0.93 for angles of attack up to 20° for several spoiler projections.

INTRODUCTION

At high subsonic speeds, most investigations of spoiler-aileron configurations have been made to determine aerodynamic forces. Limited information at these speeds shows the effect of spoilers on wing pressure distributions. (For example, see refs. 1 to 3.) There is, however, even less information pertaining to spoiler loads at high subsonic speeds (ref. 3). In order to obtain more information of this nature and to supplement reference 2, an investigation was made in the Langley high-speed 7- by 10-foot tunnel using plug- and semaphore-type spoiler ailerons at various projections on a steel semispan wing through a Mach number range from 0.60 to 0.93 and angles of attack up to 20°.

COEFFICIENTS AND SYMBOLS

S	pressure coefficient $\frac{H - p}{q}$
H	total free-stream pressure, lb/sq ft
M	free-stream Mach number
p	local static pressure, lb/sq ft
q	free-stream dynamic pressure, lb/sq ft
α	angle of attack, deg
b	wing span, in.
c	local wing chord, in.
c_{ps}	local plug-type spoiler chord (fig. 1), in.
c_{ss}	local semaphore spoiler chord (fig. 2(b)), in.
z	distance from upper edge of spoiler to orifice. (The upper edge is that part of spoiler which first emerges from wing when spoiler is deflected, in.)
l	length of any semaphore-type-spoiler segment (fig. 2(b)), in.
δ	projection of spoiler (projections above upper-wing surface are negative)
c_{n_s}	spoiler-section normal-force coefficient, $\frac{1}{c_s}\int_0^{c_s}(S_R - S_F)\,dz$
$c_{m_{t_s}}$	spoiler-section twisting-moment coefficient about spoiler upper edge, $\frac{1}{c_s^2}\int_0^{c_s}(S_R - S_F)\,-z\,dz$

Subscripts:

s	spoiler
ps	plug spoiler

ss	semaphore spoiler
w	wing
R	rear spoiler surface
F	front spoiler surface

MODEL AND APPARATUS

The sweptback semispan-wing model used in this investigation was mounted vertically in the Langley high-speed 7- by 10-foot tunnel with the ceiling serving as a reflection plane. (The height of the test section is 7 feet.)

The geometric characteristics and dimensions of the wing and spoiler configurations are presented in figures 1 and 2. The steel wing was swept back 35° at the quarter-chord line, had an aspect ratio of 4, a taper ratio of 0.6, NACA 65A006 airfoil sections parallel to the free stream, and neither twist nor dihedral.

The center line of the plug-type spoiler coincided with the 70-percent wing-chord line and deflections were obtained by rotating about the 60-percent wing-chord line (fig. 1). Pressure orifices were located on the upper and lower edges as well as on the front and rear faces of the spoiler at three spanwise stations. The positions of the orifices on the spoiler faces are given for each station in table I.

The semaphore-type spoilers were located also along the 70-percent wing-chord line although each segment was skewed 19.5° forward. (See fig. 2(a).) Deflections of these spoilers were obtained by rotating them about an axis in the plane of the wing chord and normal to the face of each segment. Pressure orifices were located on the upper and lower edges as well as on the front and rear faces of one segment at three stations along its length (fig. 2(b)). The positions of the orifices on the spoiler for each station are given in table II.

TESTS

The tests were made in the Langley high-speed 7- by 10-foot tunnel through the Mach number range from 0.60 to 0.93.

The plug spoiler was tested at projections of 0, -0.02c, -0.04c (gap unsealed), and -0.04c (gap sealed) through a maximum angle-of-attack

range from 0° to 20°. Tests were made with all semaphore spoilers undeflected and deflected to -15° and -30° through a maximum angle-of-attack range from 0° to 20° and deflected to -45° through a maximum angle-of-attack range from -20° to 20°. In addition, a single semaphore spoiler deflected to -45° was tested through a maximum angle-of-attack range from -20° to 20°. The Reynolds number varied from about 3.1×10^6 at $M = 0.60$ to about 4.0×10^6 at $M = 0.93$.

PRESENTATION OF DATA

In order to expedite the publication of the data, the pressure distributions and the integrated section force and moment data are being presented without discussion. It is felt, however, that the data as presented will be useful in the prediction of the spoiler loads for spoiler configurations similar to those of this investigation. The data have been corrected for stream misalinement and blockage. No other tunnel-wall or reflection-plane corrections have been applied to the data. The data of reference 3 indicate that reflection-plane effects on the spoiler loading are probably small. The data are presented in figures 3 to 8 and an index to the data presented is given in table III.

Inasmuch as the model was symmetrical, the tests at negative angles of attack with negative spoiler projections may be considered as tests made at positive angles of attack with positive spoiler projections with due regard to signs.

Langley Aeronautical Laboratory,
National Advisory Committee for Aeronautics,
Langley Field, Va., May 27, 1954.

REFERENCES

1. Luoma, Arvo A.: An Investigation of the Lateral-Control Characteristics of Spoilers on a High-Aspect-Ratio Wing of NACA 65-210 Section in the Langley 8-Foot High-Speed Tunnel. NACA RM L7D21, 1947.

2. Hammond, Alexander D., and McMullan, Barbara M.: Chordwise Pressure Distribution at High Subsonic Speeds Near Midsemispan of a Tapered 35° Sweptback Wing of Aspect Ratio 4 Having NACA 65A006 Airfoil Sections and Equipped With Various Spoiler Ailerons. NACA RM L52C28, 1952.

3. Hallissy, Joseph M., Jr., West F. E., Jr., and Liner, George: Effects of Spoiler Ailerons on the Aerodynamic Load Distribution Over a 45° Sweptback Wing At Mach Numbers From 0.60 to 1.03. NACA RM L54C17a, 1954.

TABLE I

LOCATION OF PRESSURE ORIFICES ON PLUG SPOILERS

[Orifices on upper and lower edges of spoiler at all spanwise positions]

Chordwise position on front face, z/c_{ps}	Chordwise position on rear face, z/c_{ps}
0.20b/2 station	
0.184	0.167
---	.341
.514	.501
.663	.663
.831	.831
0.46b/2 station	
0.212	0.216
.375	.360
.492	.502
.625	.636
.784	.784
0.65b/2 station	
0.185	0.185
---	.400
.575	.579
.785	.785

TABLE II

LOCATION OF PRESSURE ORIFICES ON SEMAPHORE SPOILER

[Orifices on upper and lower edges of spoiler at all orifice stations]

Chordwise position on front face, z/c_{ss}	Chordwise position on rear face, z/c_{ss}
0.42l station	
0.091	0.099
.258	.251
.391	----
.555	----
.702	.712
.910	.854
0.62l station	
0.132	0.127
.299	.299
.429	----
.604	.608
.737	.752
----	.962
0.81l station	
0.026	0.033
.193	.216
.350	.366
.500	----
.636	.663
.858	.856

TABLE III

INDEX TO DATA PRESENTED

[Data taken at Mach numbers of 0.60, 0.80, 0.90, and 0.93]

Figure	Variation of -	Type of spoiler	Station	Deflection range
3	S with z/c_{ps}	Plug-type	0.20b/2, 0.46b/2, and 0.65b/2	0, -0.02c, and -0.04c (sealed and unsealed)
4	S with z/c_{ss}	Semaphore-type	0.42l, 0.62l, and 0.81l	0°, -15°, -30°, and -45°
5	S with z/c_{ss}	Semaphore-type	0.42l, 0.62l, and 0.81l	-45°
6	C_n with α	Plug-type	0.20b/2, 0.46b/2, and 0.65b/2	0, -0.02c, and -0.04c (sealed and unsealed)
7	C_{m_t} with α	Plug-type	0.20b/2, 0.46b/2, and 0.65b/2	0, -0.02c, and -0.04c (sealed and unsealed)
8	C_n with α	Semaphore-type	0.42l, 0.62l, and 0.81l	0°, -15°, -30°, and -45°
9	C_{m_t} with α	Semaphore-type	0.42l, 0.62l, and 0.81l	0°, -15°, -30°, and -45°

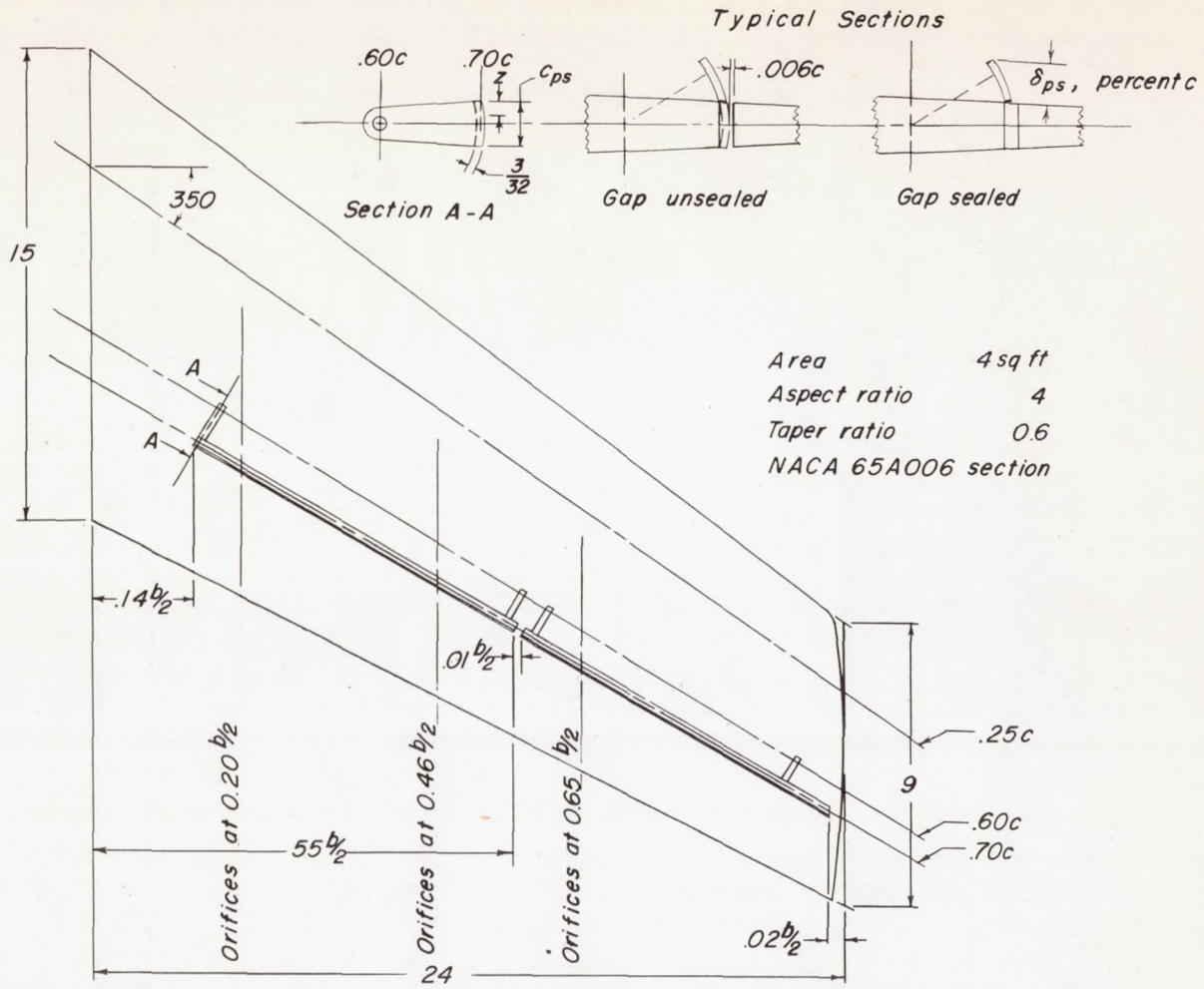

Figure 1.- Geometric characteristics of a 35° sweptback semispan wing with plug-type spoiler ailerons and the spanwise location of the pressure orifices on the spoiler. (All dimensions are in inches unless otherwise indicated.)

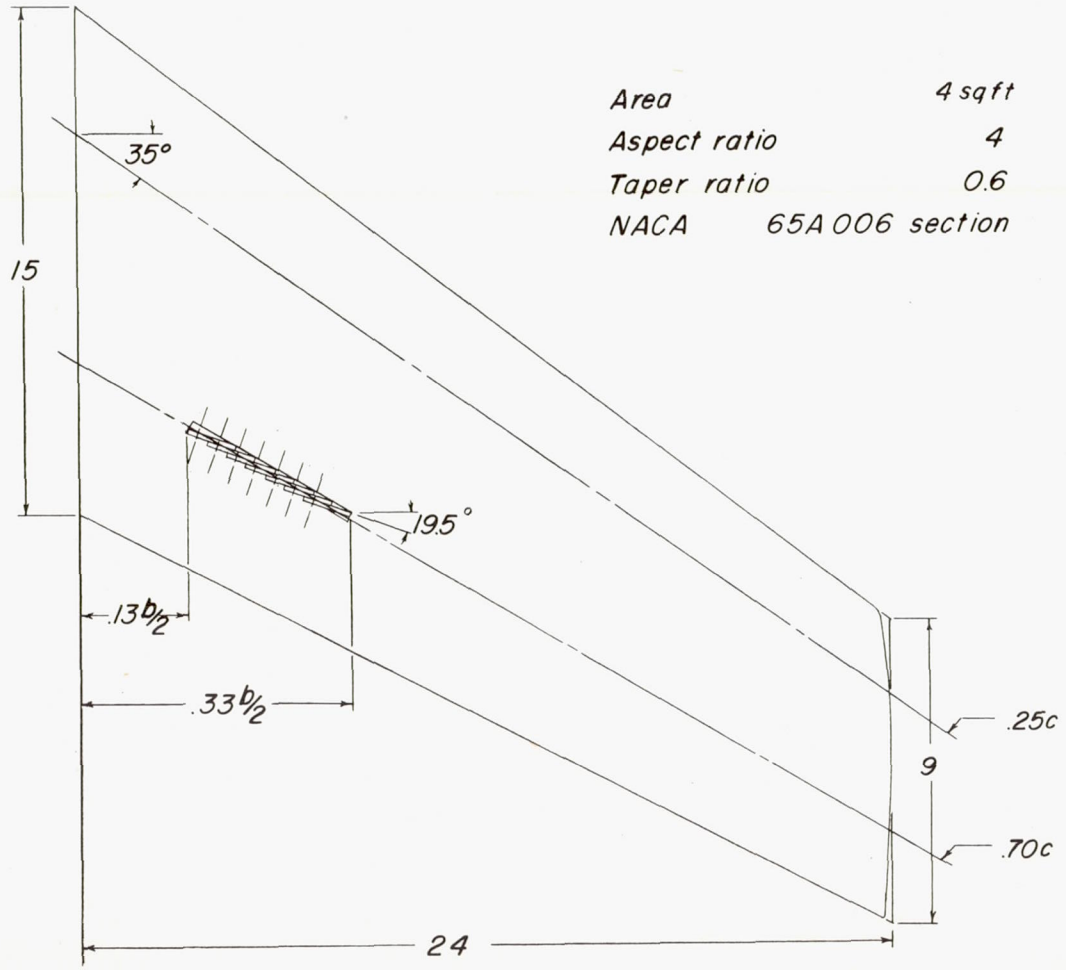

(a) Location of semaphore spoilers.

Figure 2.- Geometric characteristics of the 35° sweptback wing equipped with semaphore-type spoiler ailerons. (All dimensions are in inches unless otherwise noted.)

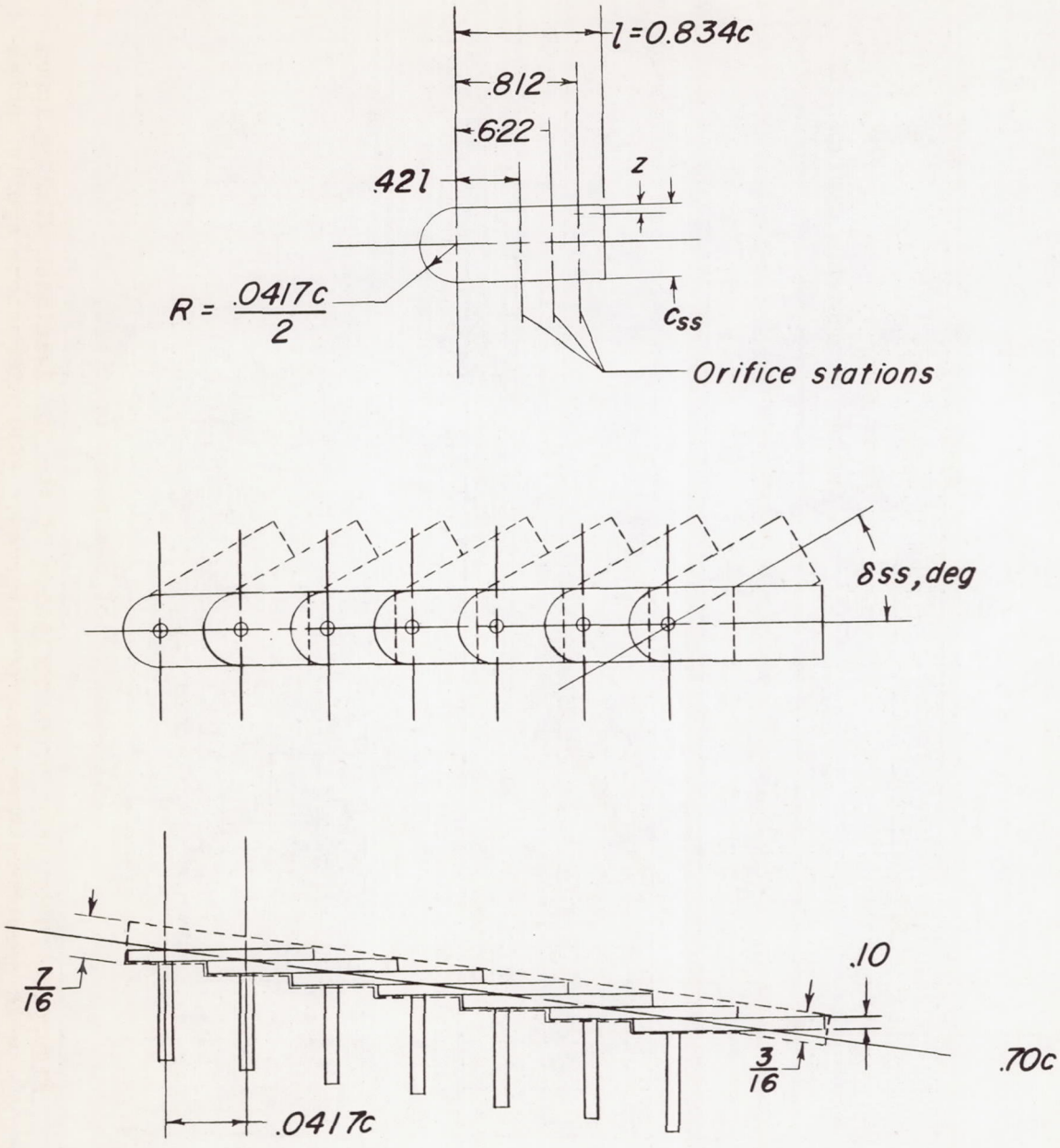

(b) Details of semaphore spoilers.

Figure 2.- Concluded.

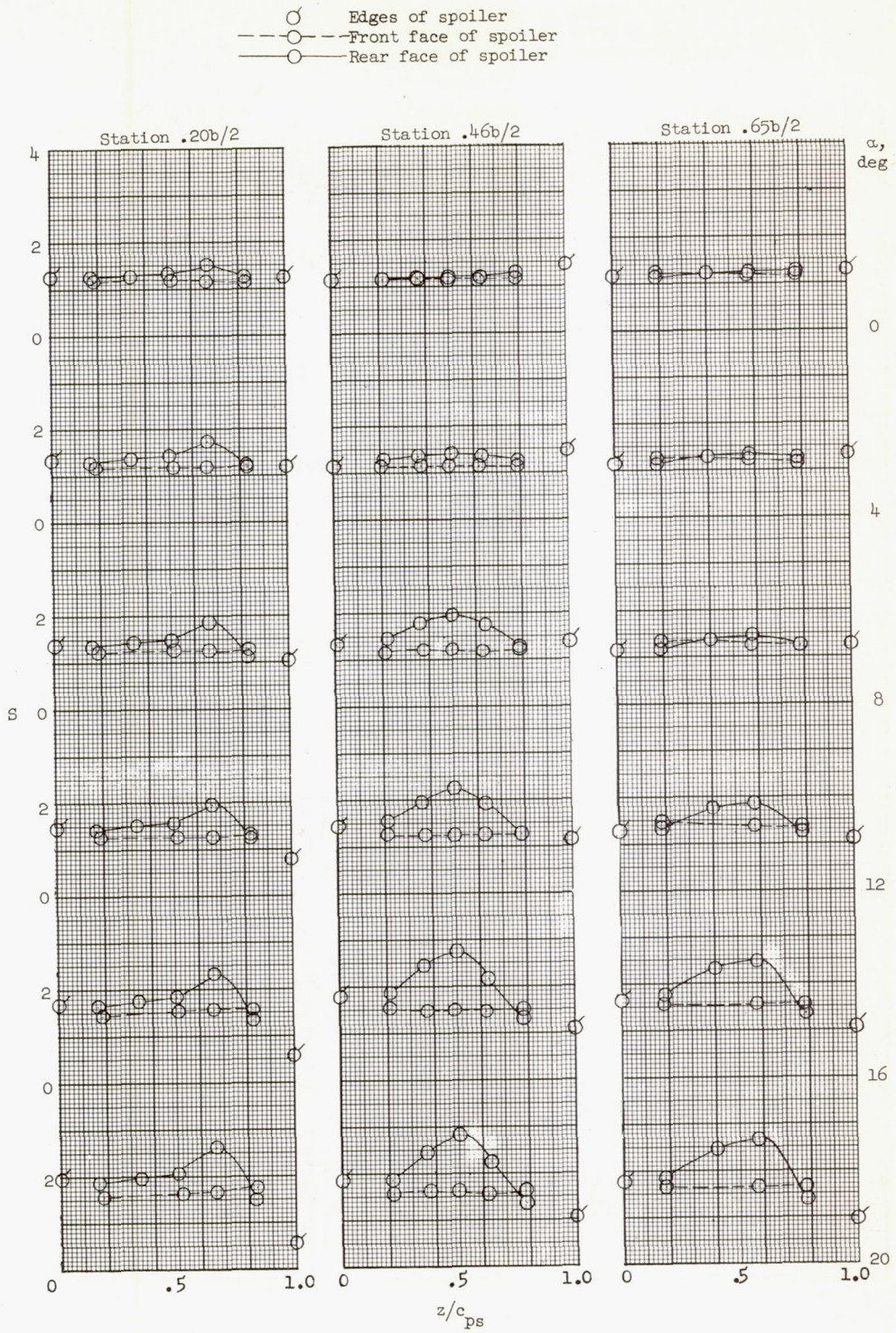

(a) $M = 0.60$; $\delta_{ps} = 0$.

Figure 3.- Pressure coefficient on the plug spoilers at three spanwise stations.

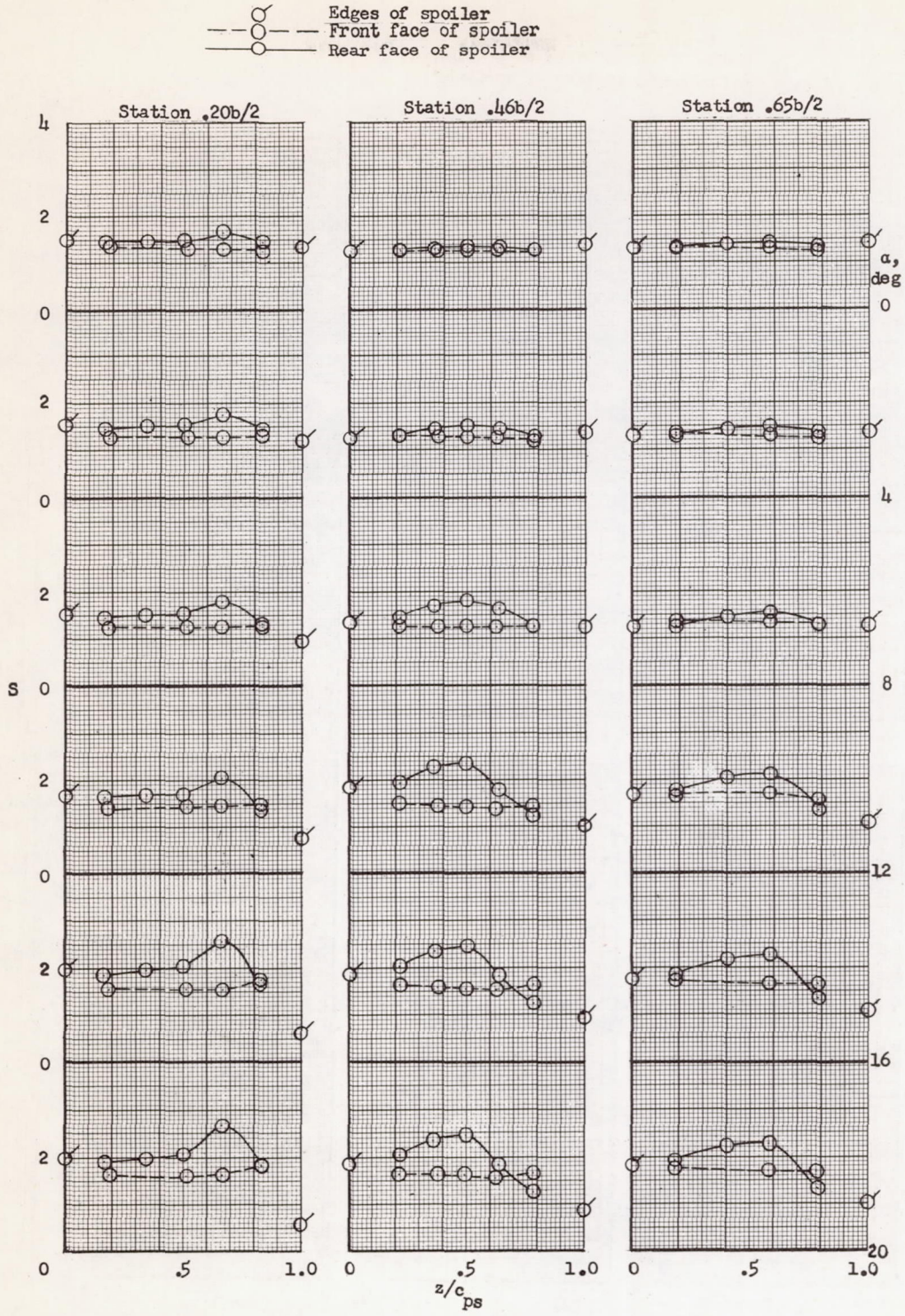

(b) M = 0.80; δ_{ps} = 0.

Figure 3.- Continued.

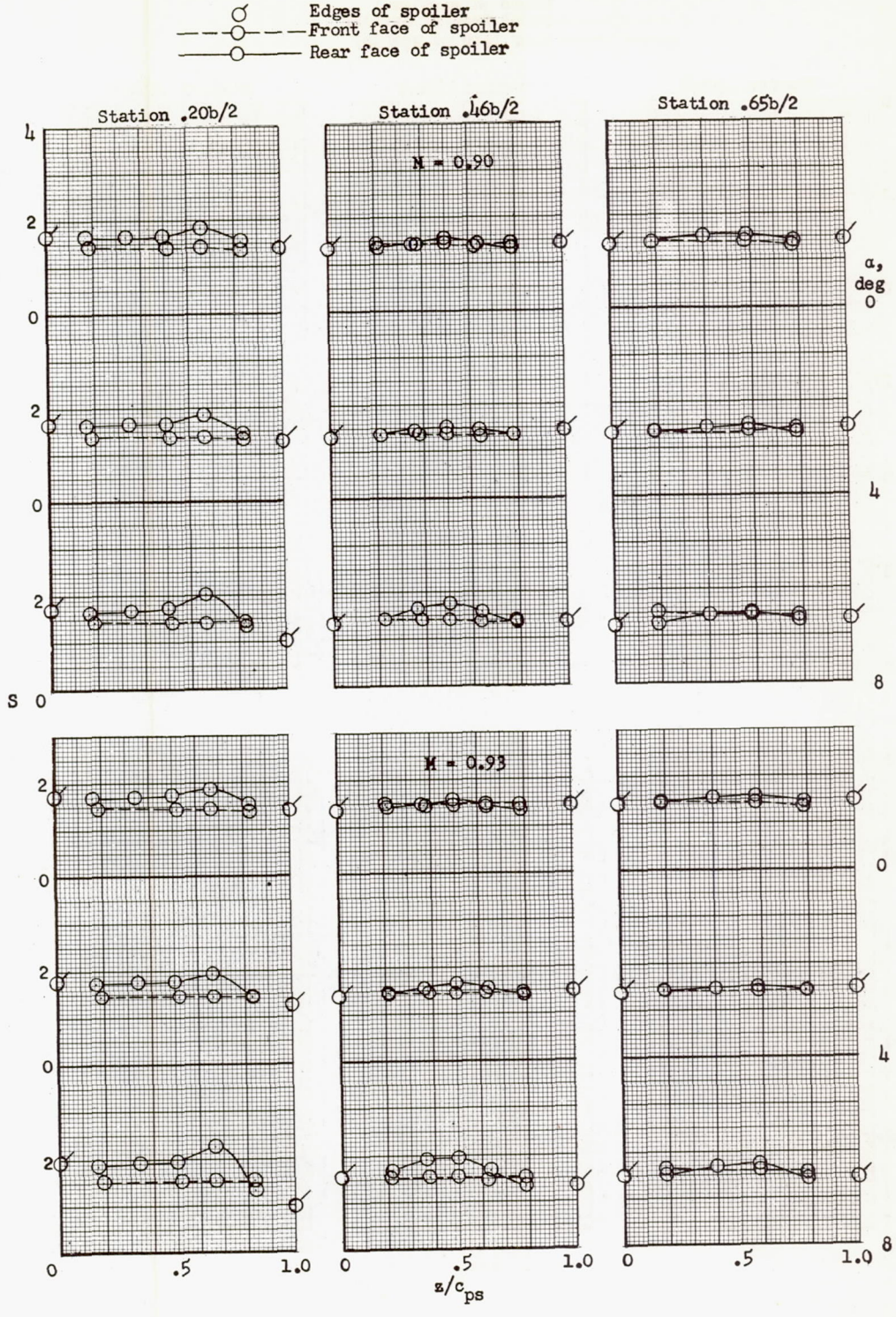

(c) M = 0.90, 0.93; δ_{ps} = 0.

Figure 3.- Continued.

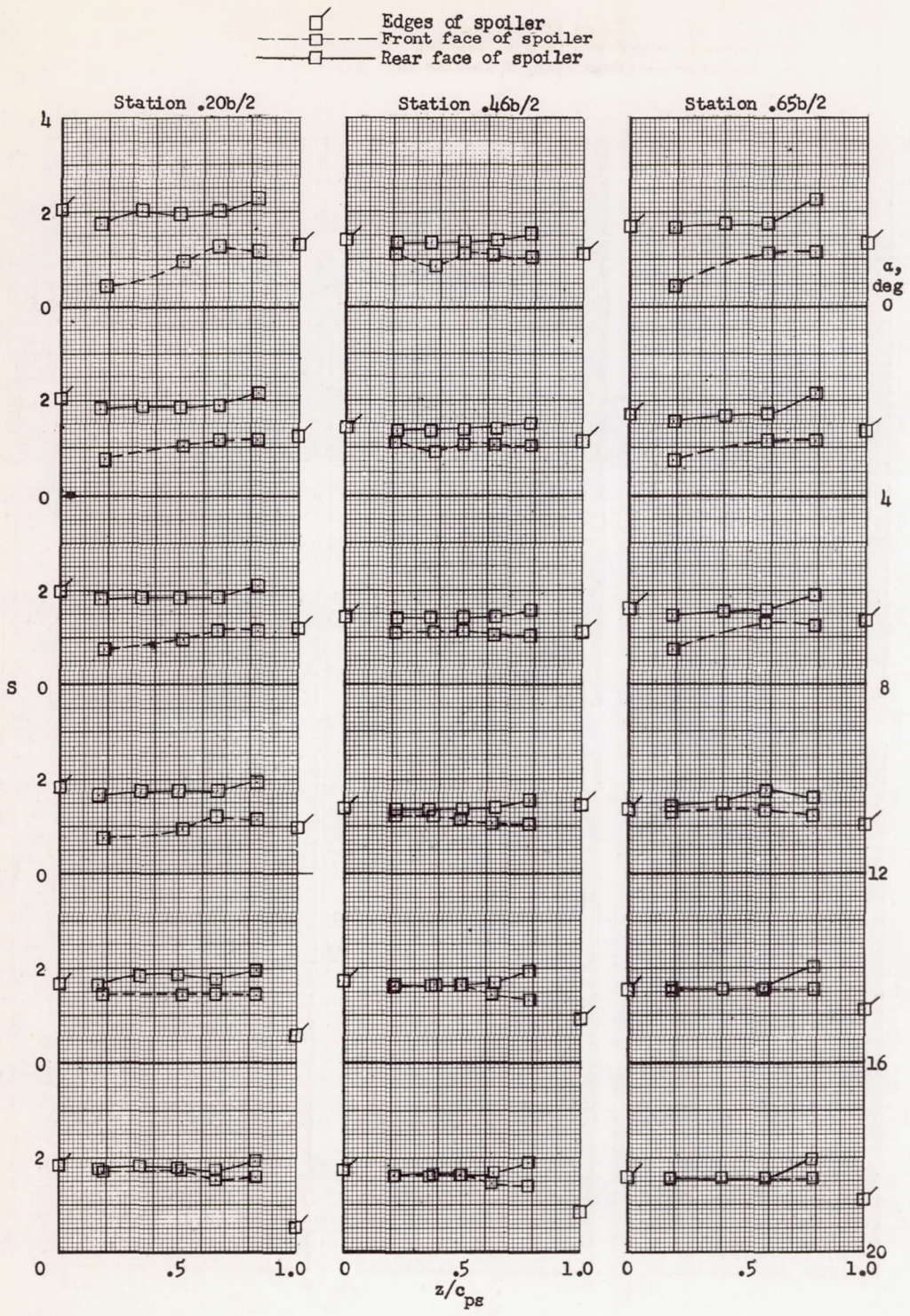

(d) M = 0.60; δ_{ps} = -0.02c.

Figure 3.- Continued.

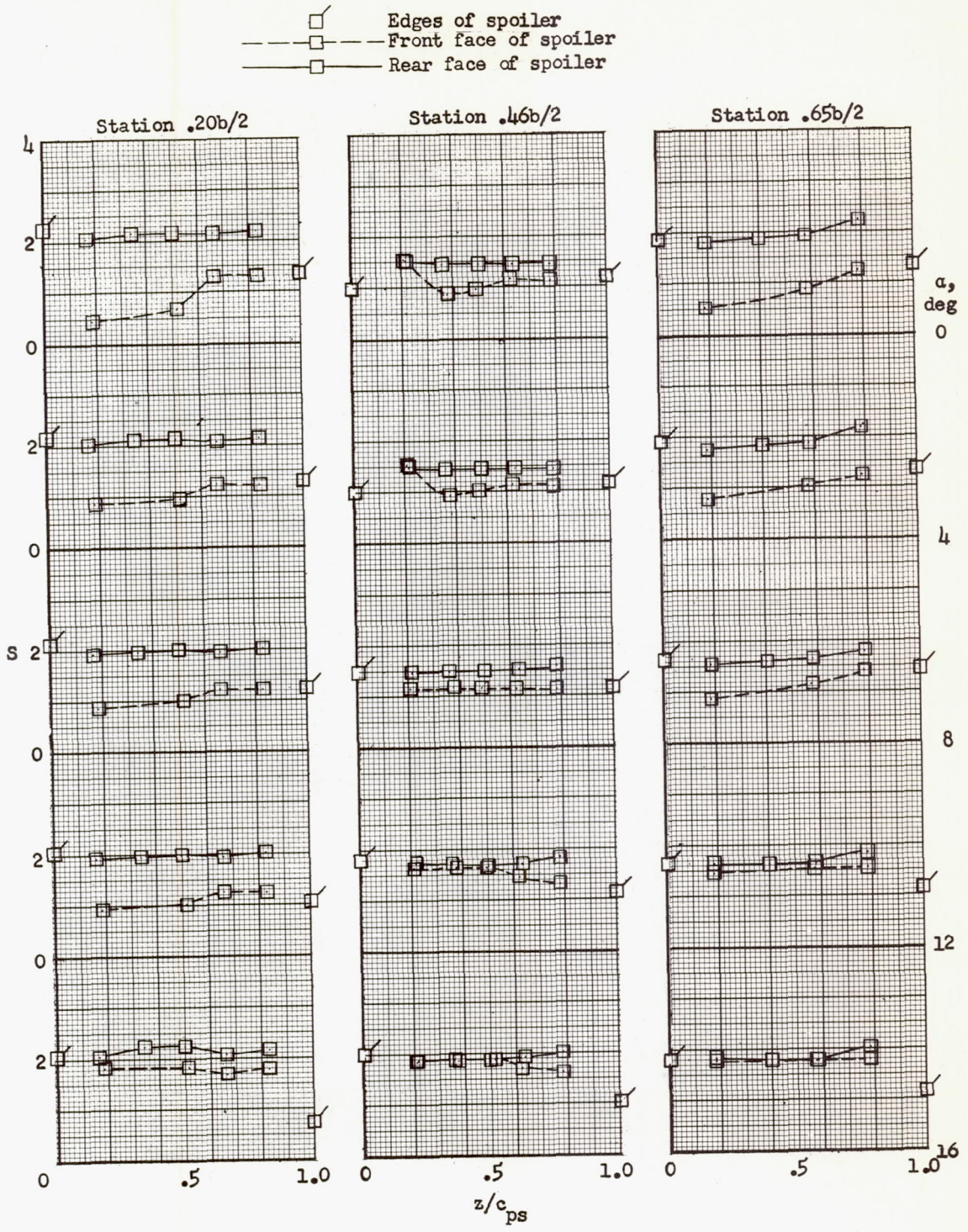

(e) M = 0.80; δ_{ps} = -0.02c.

Figure 3.- Continued.

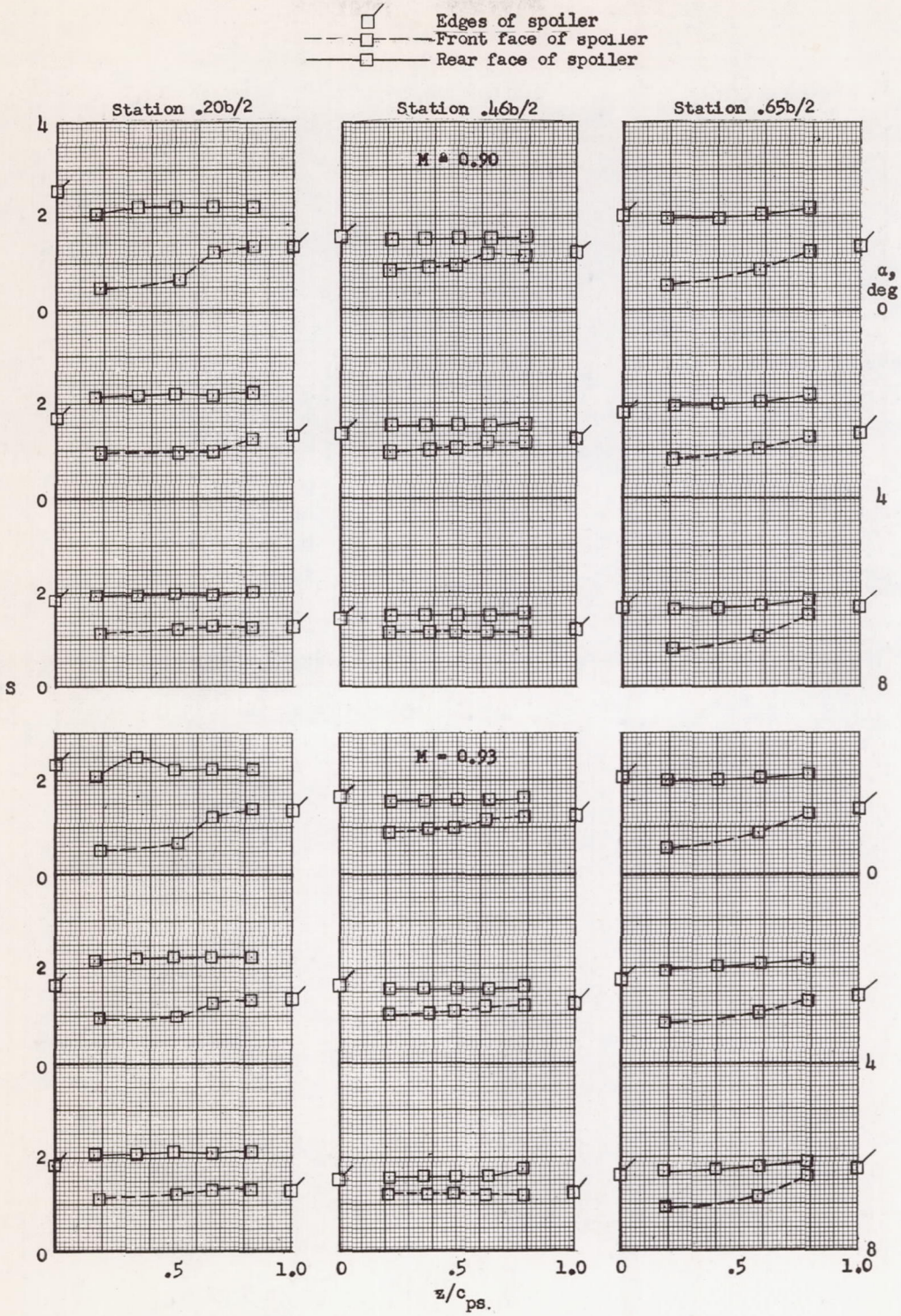

(f) M = 0.90, 0.93; δ_{ps} = -0.02c.

Figure 3.- Continued.

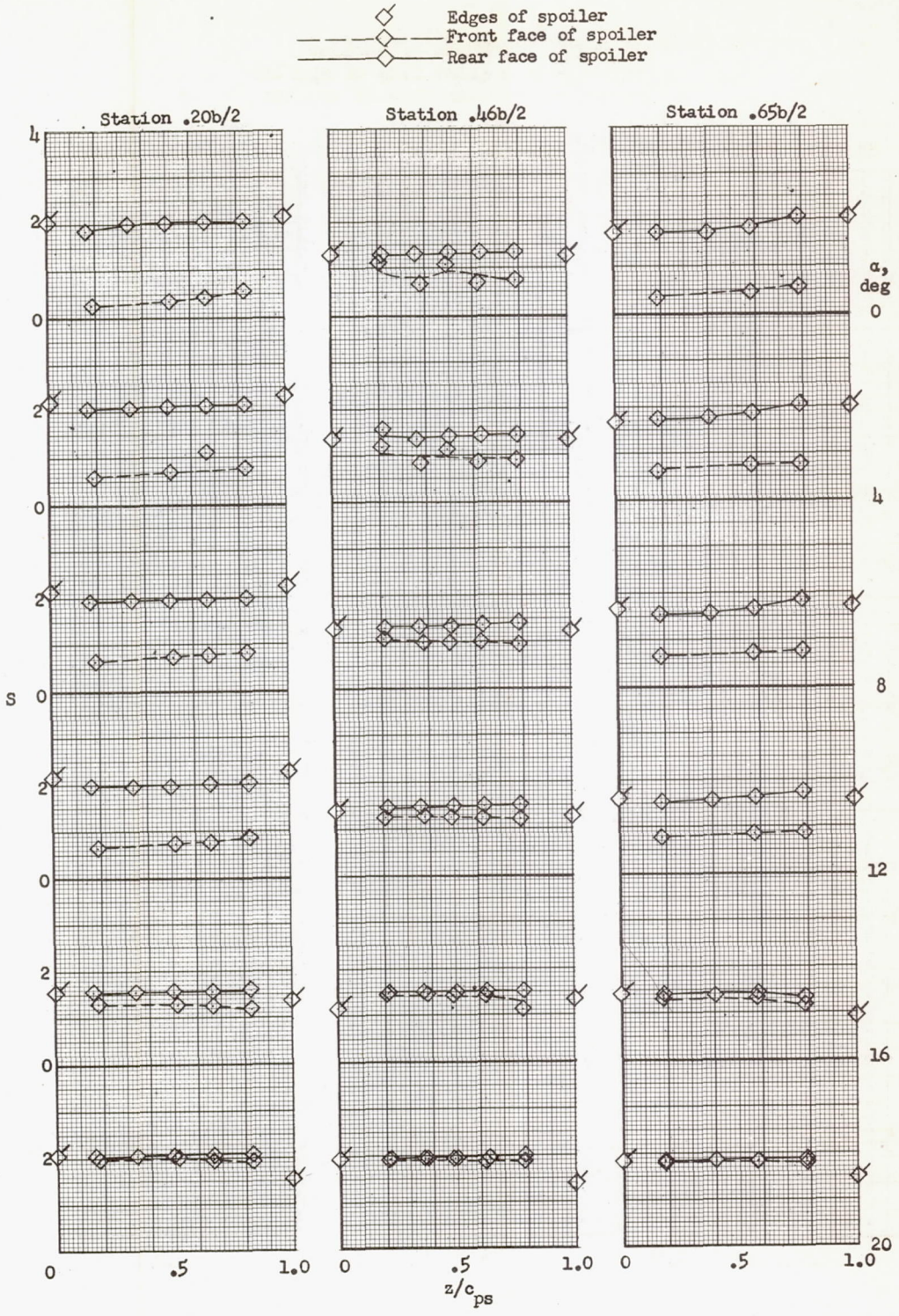

(g) M = 0.60; δ_{ps} = -0.04c; gap unsealed.

Figure 3.- Continued.

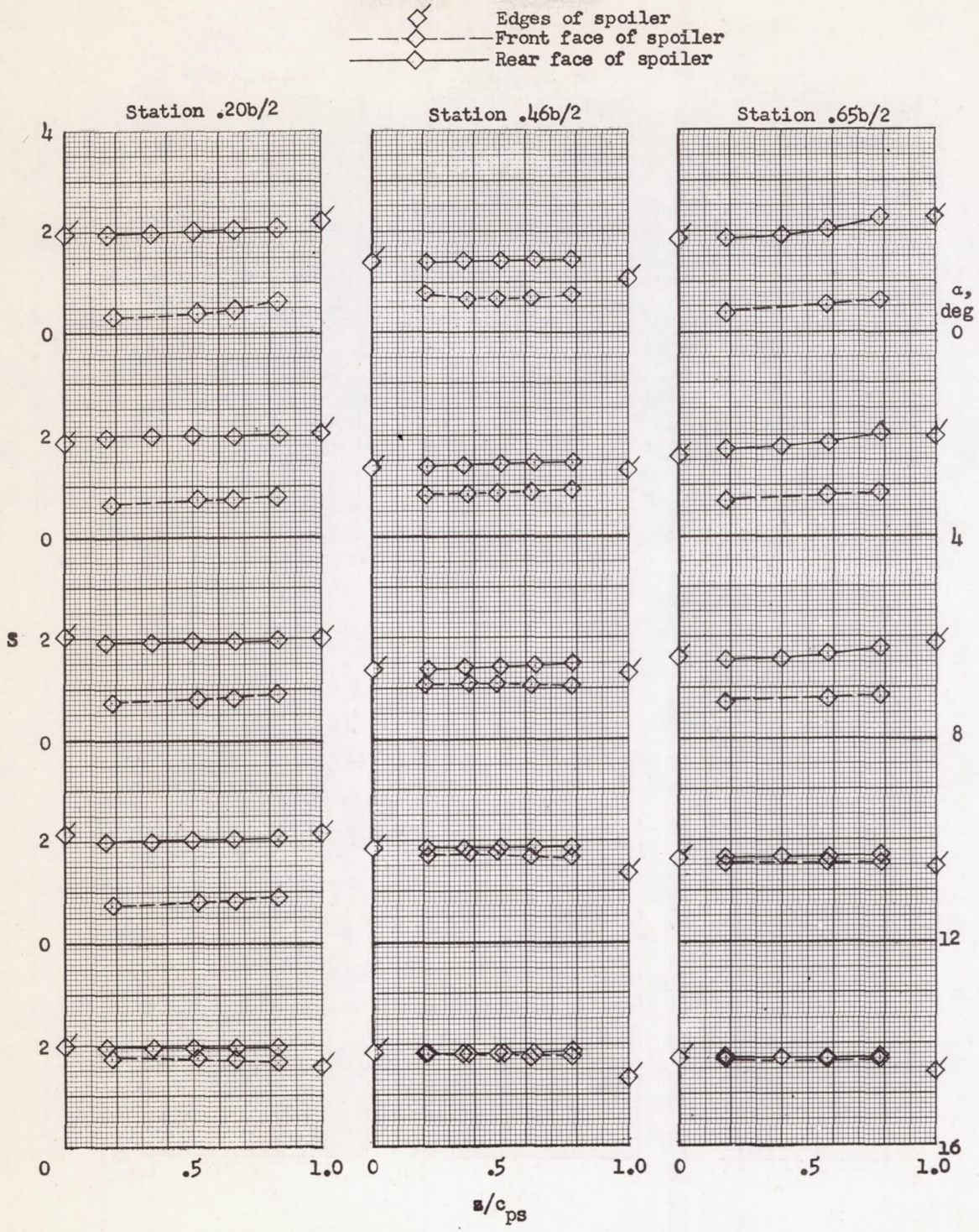

(h) M = 0.80; δ_{ps} = -0.04c; gap unsealed.

Figure 3.- Continued.

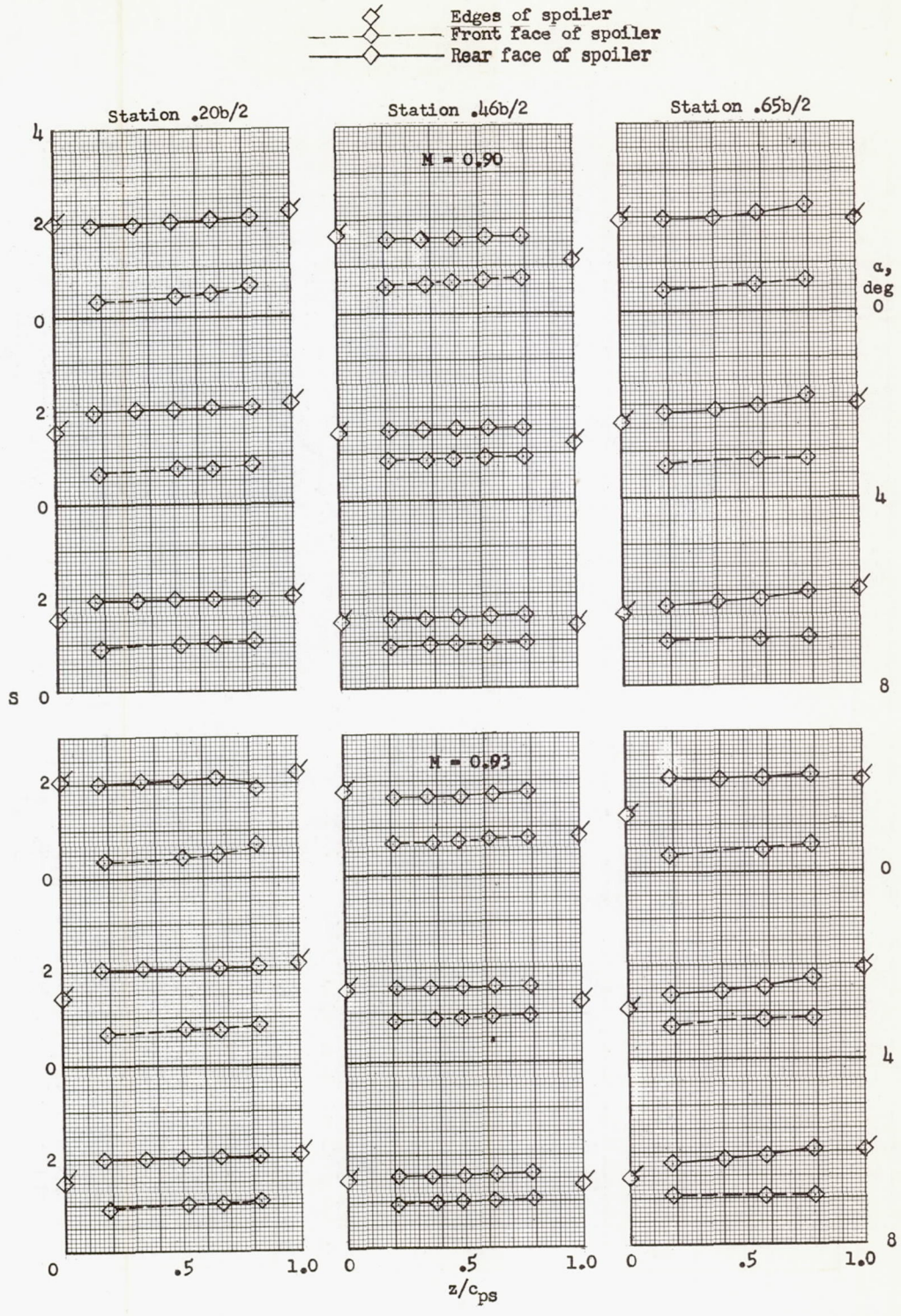

(i) M = 0.90, 0.93; δ_{ps} = -0.04c; gap unsealed.

Figure 3.- Continued.

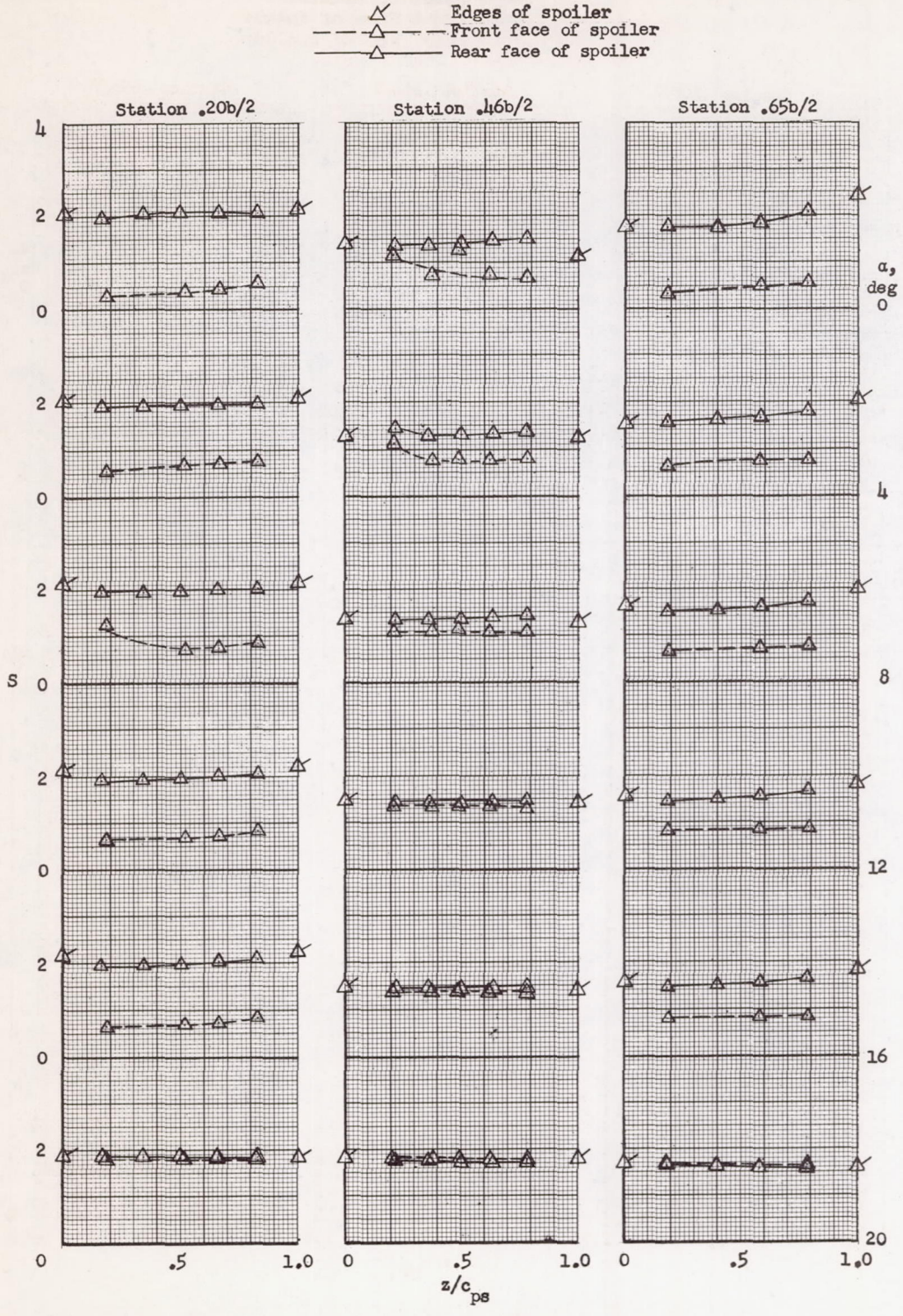

(j) M = 0.60; δ_{ps} = -0.04c; gap sealed.

Figure 3.- Continued.

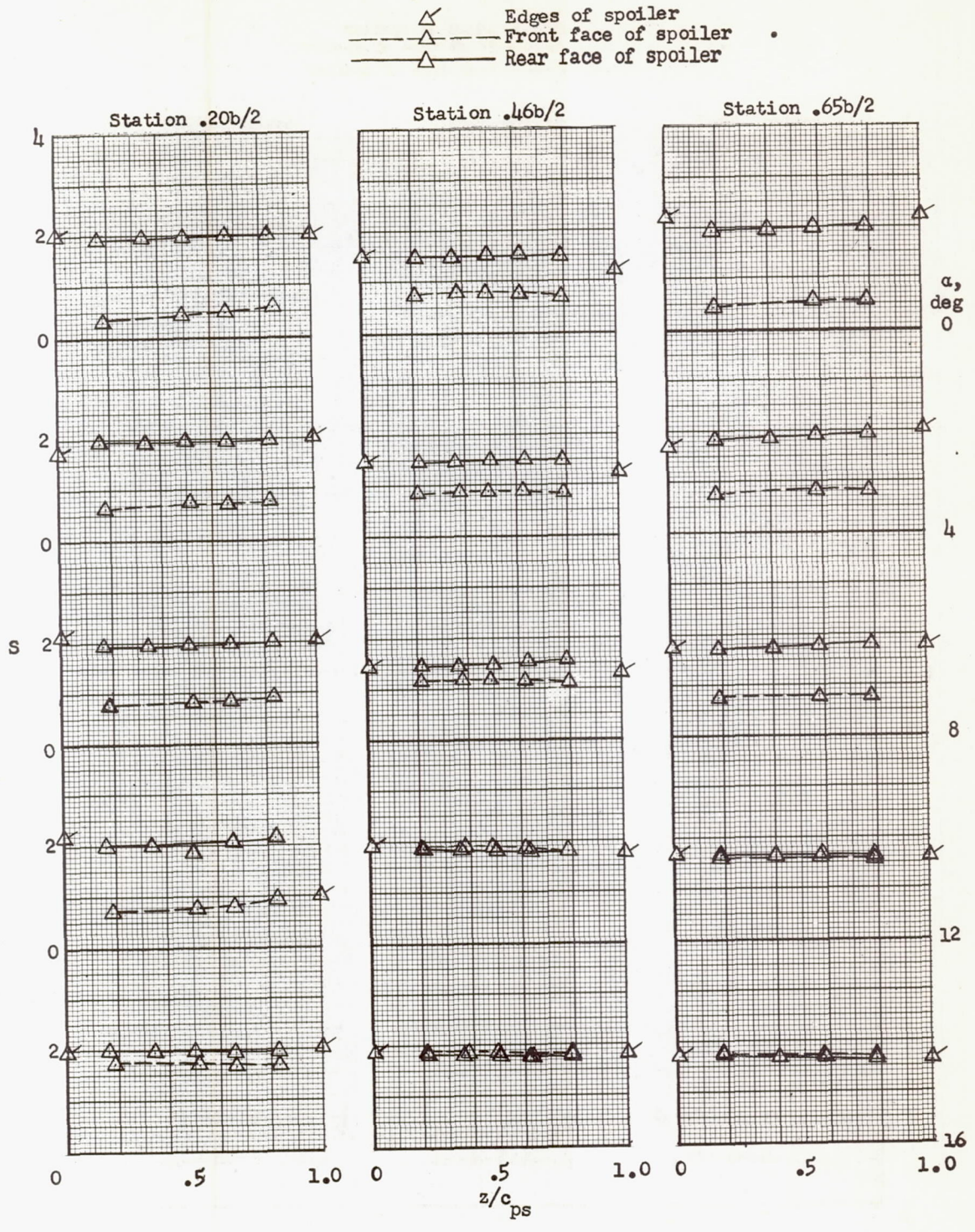

(k) M = 0.80; δ_{ps} = -0.04c; gap sealed.

Figure 3.- Continued.

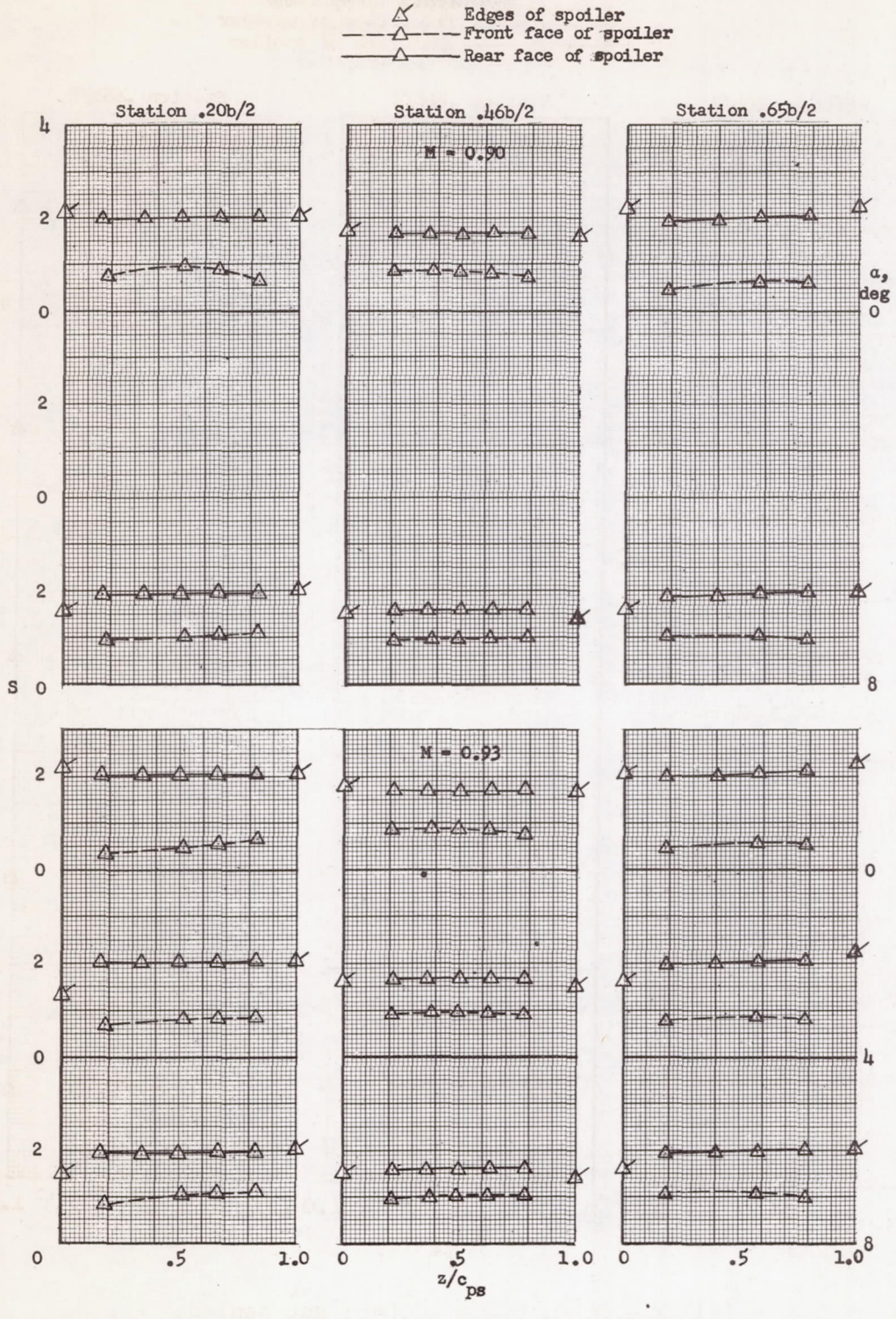

(*l*) M = 0.90, 0.93; δ_{ps} = -0.04c; gap sealed.

Figure 3.- Concluded.

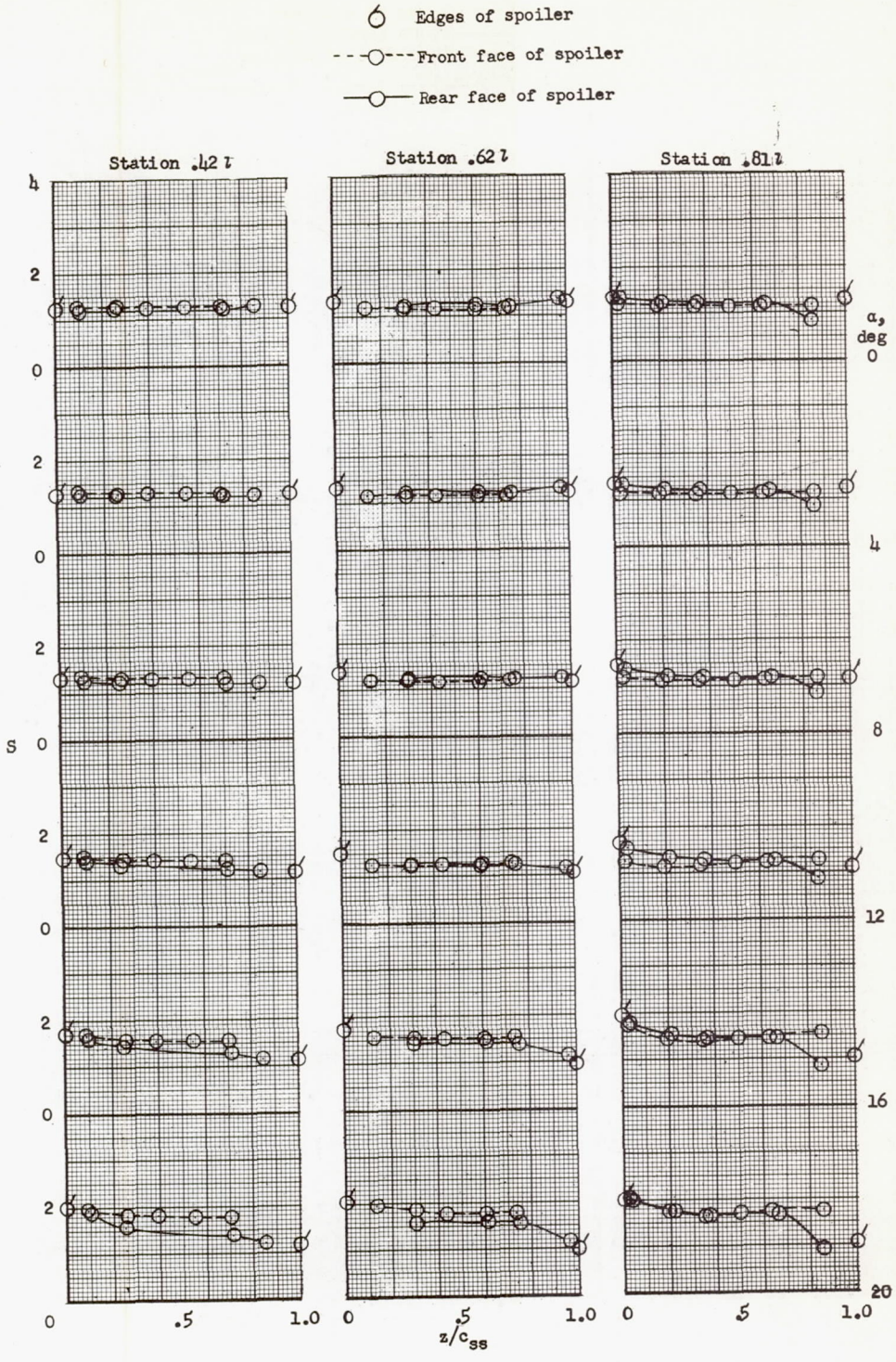

(a) M = 0.60; $\delta_{ss} = 0^{\circ}$.

Figure 4.- Pressure coefficient on a semaphore spoiler at three stations on the spoiler. All spoilers are at same deflection angle.

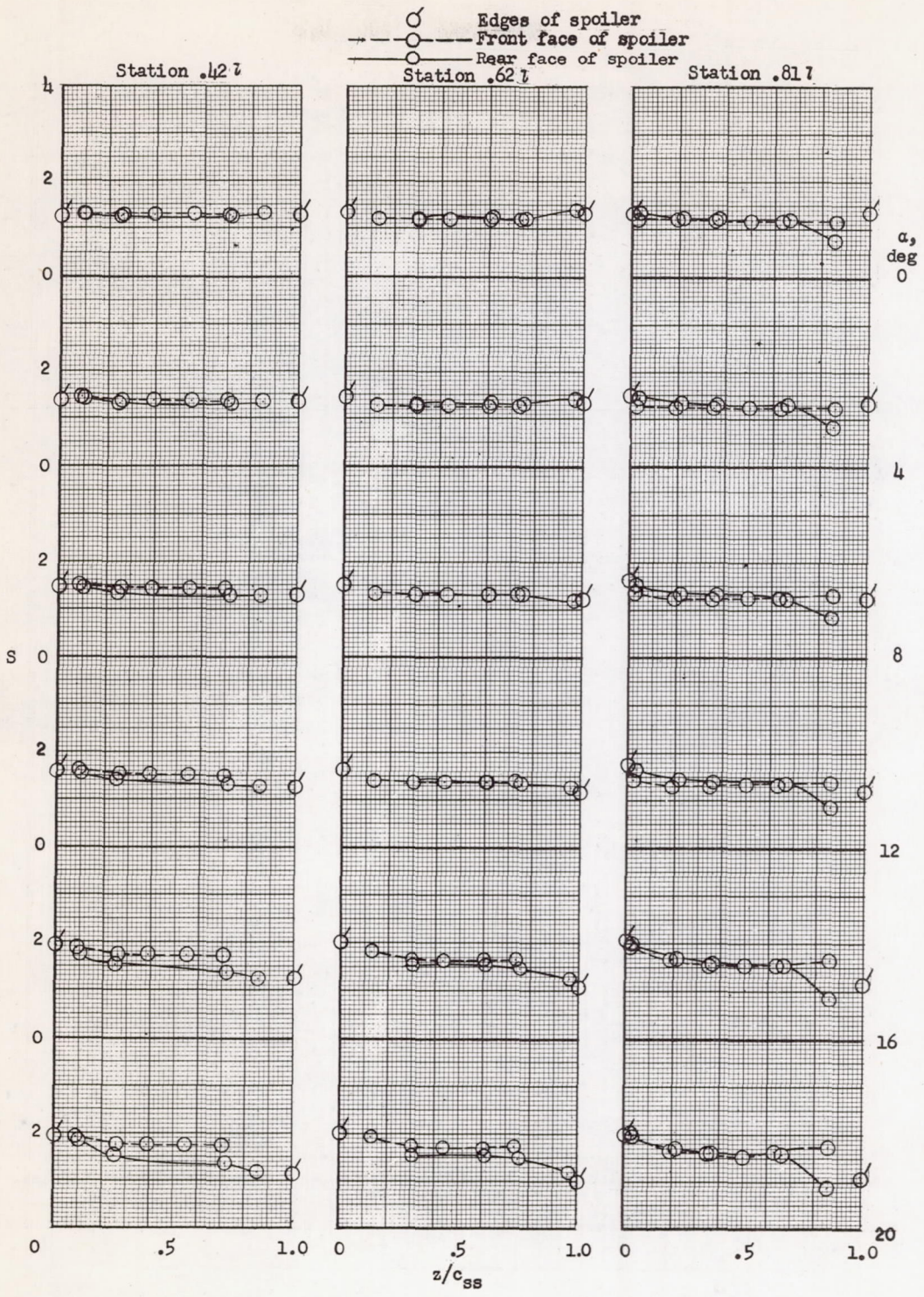

(b) M = 0.80; $\delta_{ss} = 0^{\circ}$.

Figure 4.- Continued.

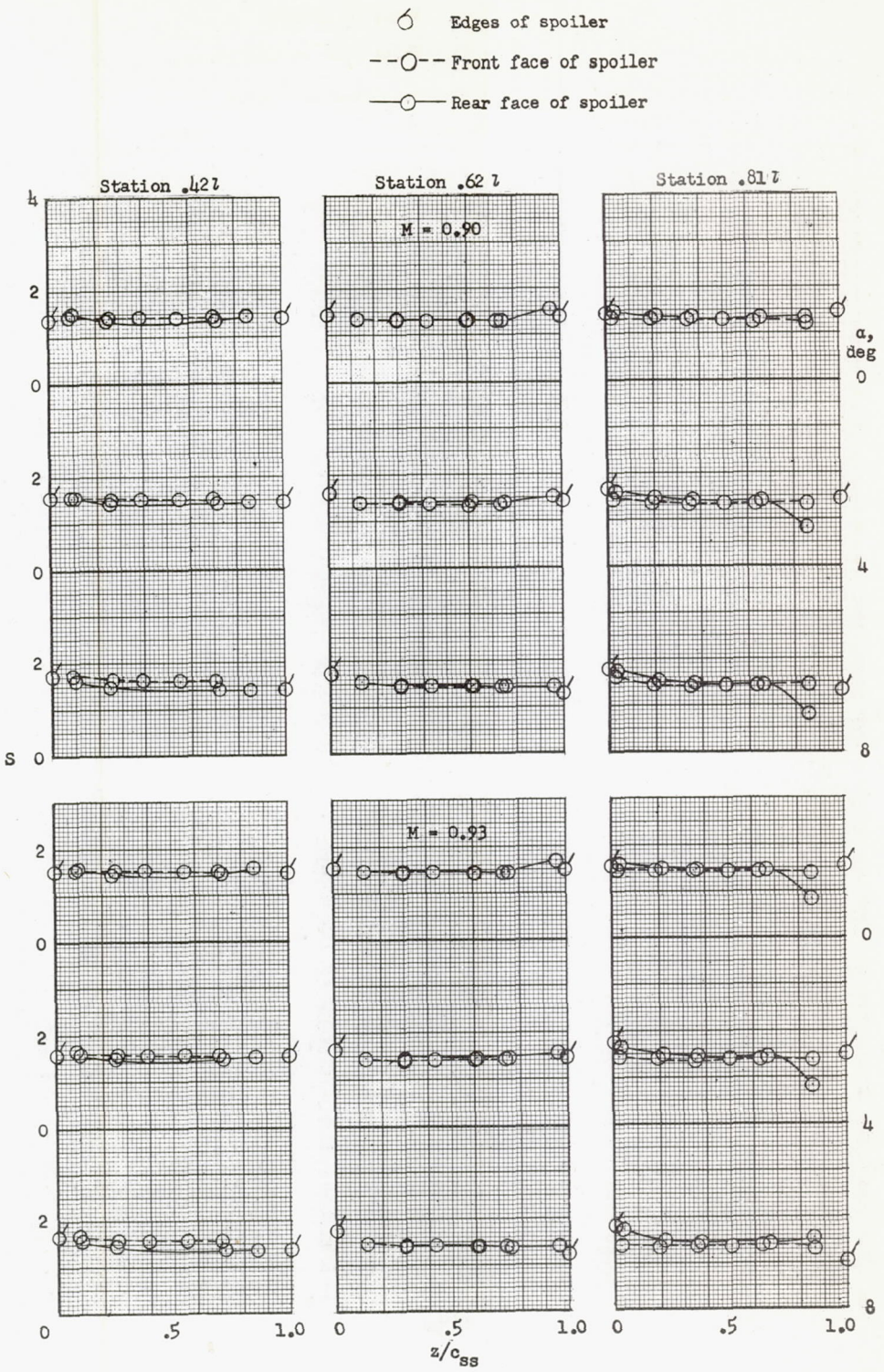

(c) M = 0.90, 0.93; $\delta_{ss} = 0^{\circ}$.

Figure 4.- Continued.

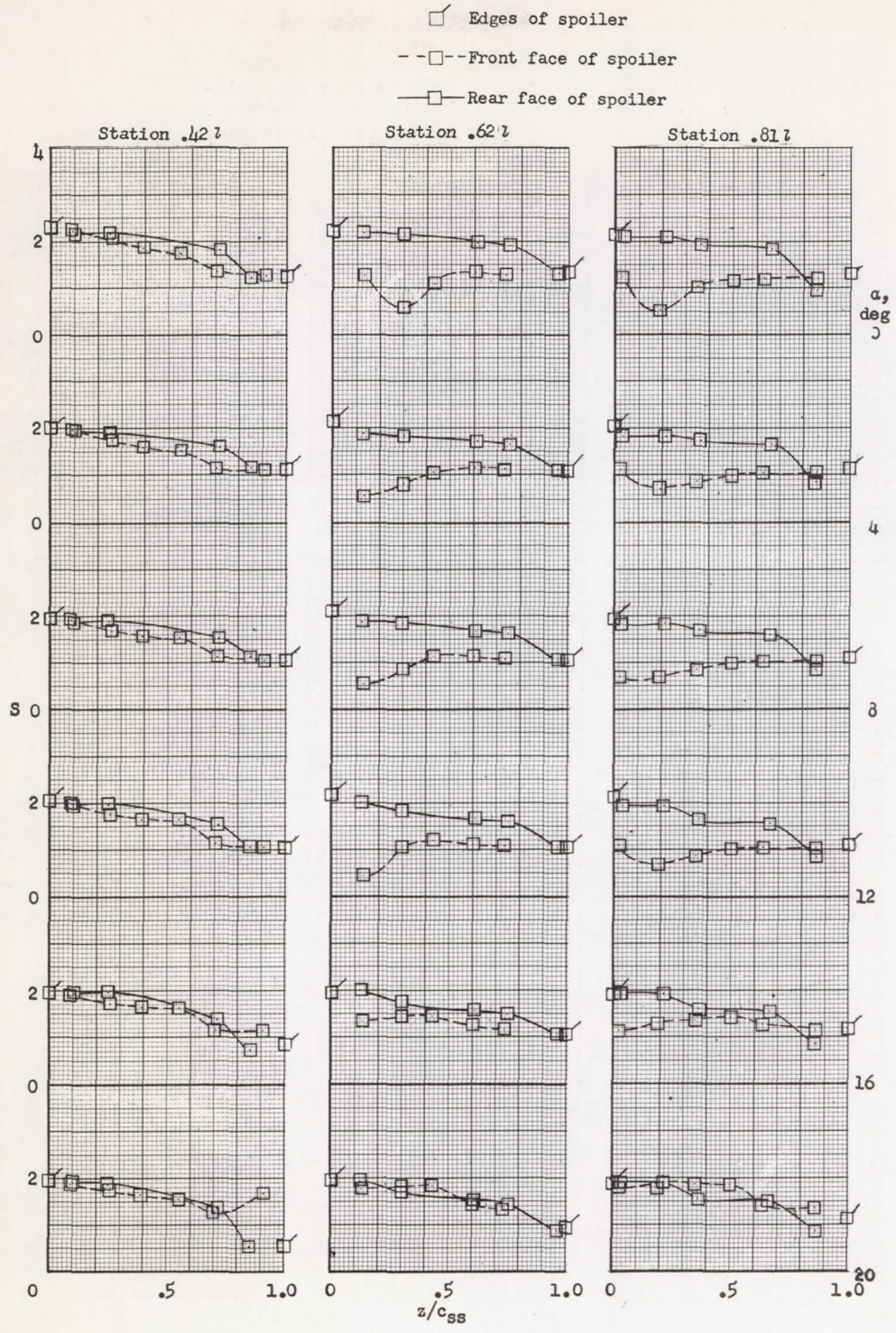

(d) M = 0.60; δ_{ss} = -15°.

Figure 4.- Continued.

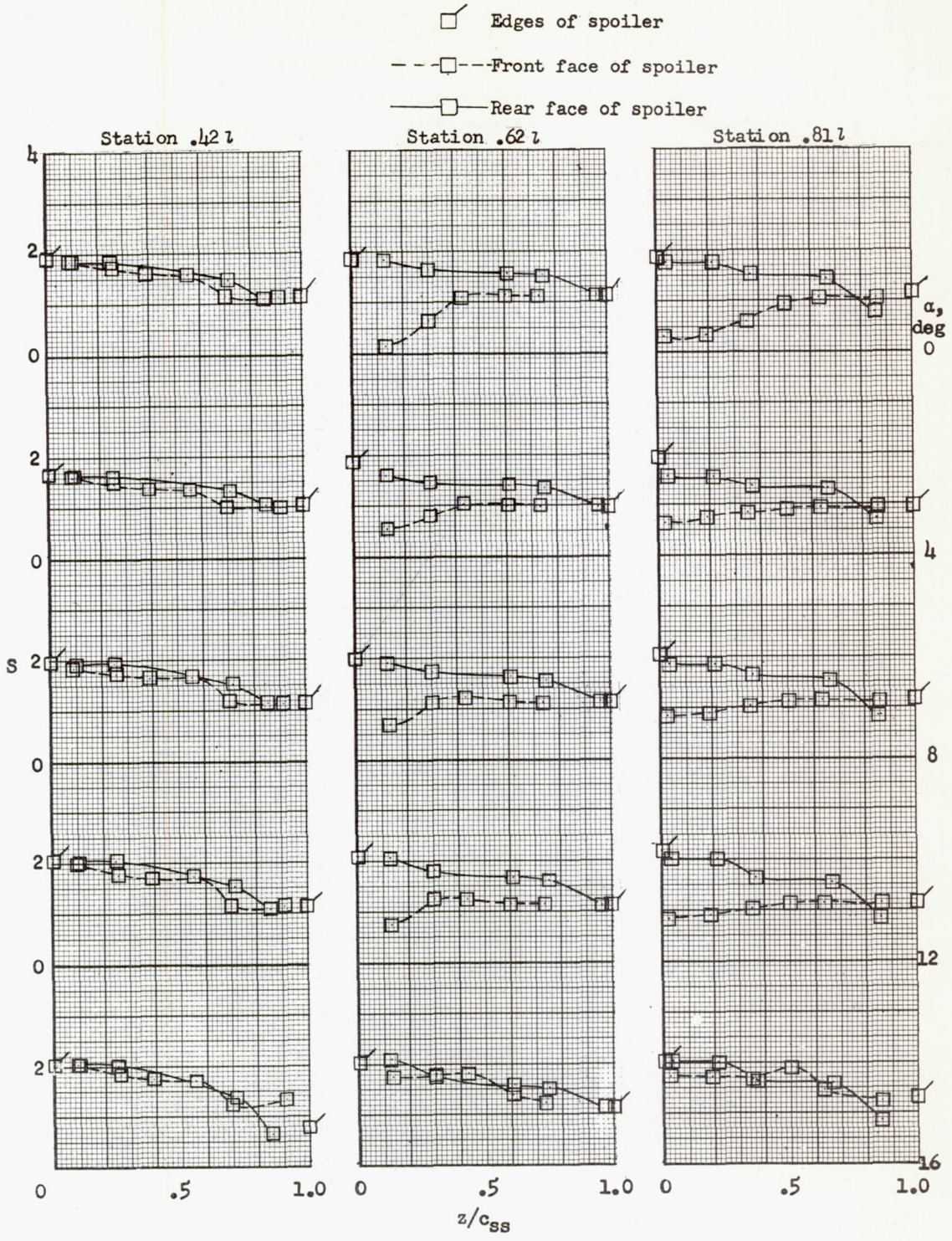

(e) M = 0.80; δ_{ss} = -15°.

Figure 4.- Continued.

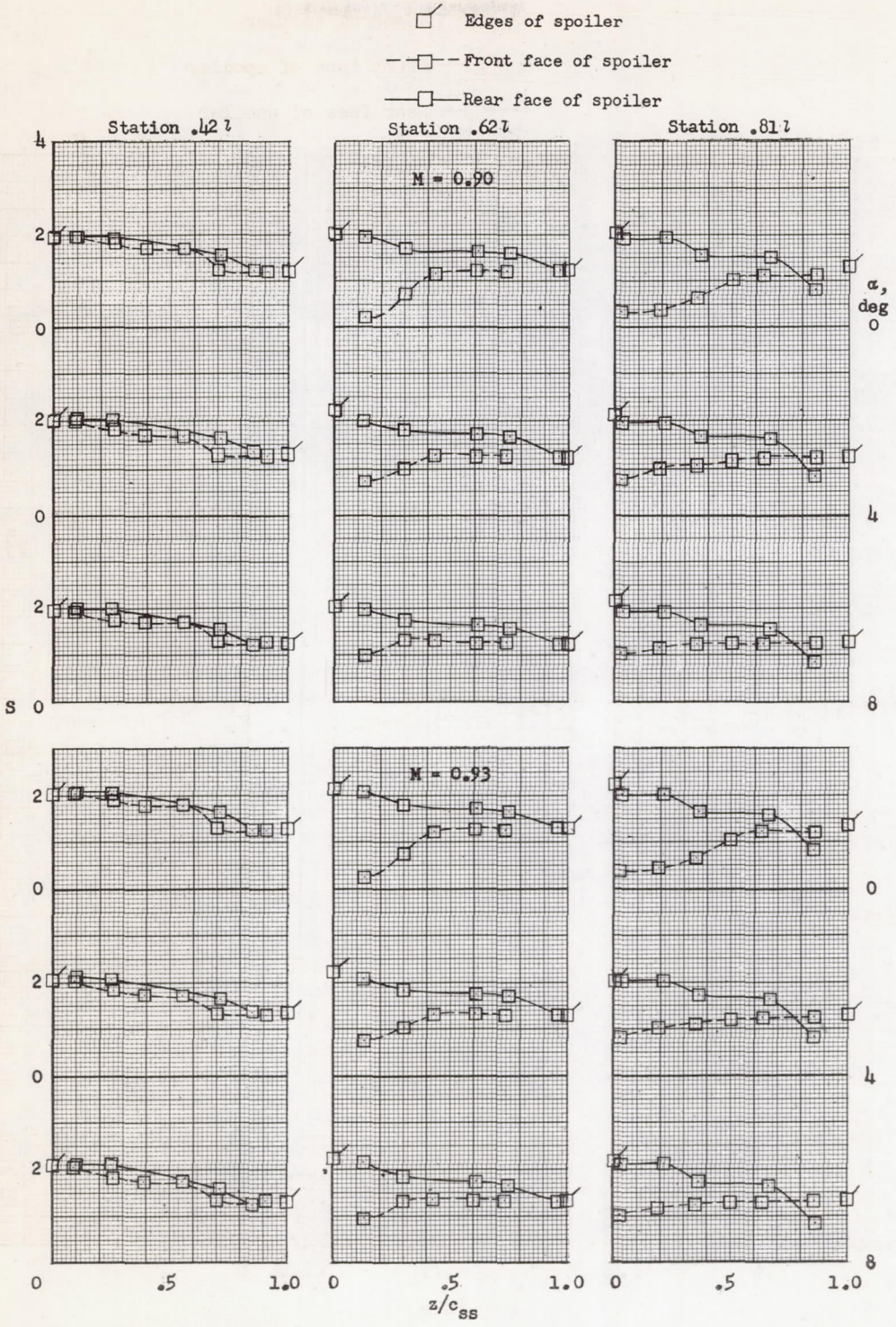

(f) M = 0.90, 0.93; δ_{ss} = -15°.

Figure 4.- Continued.

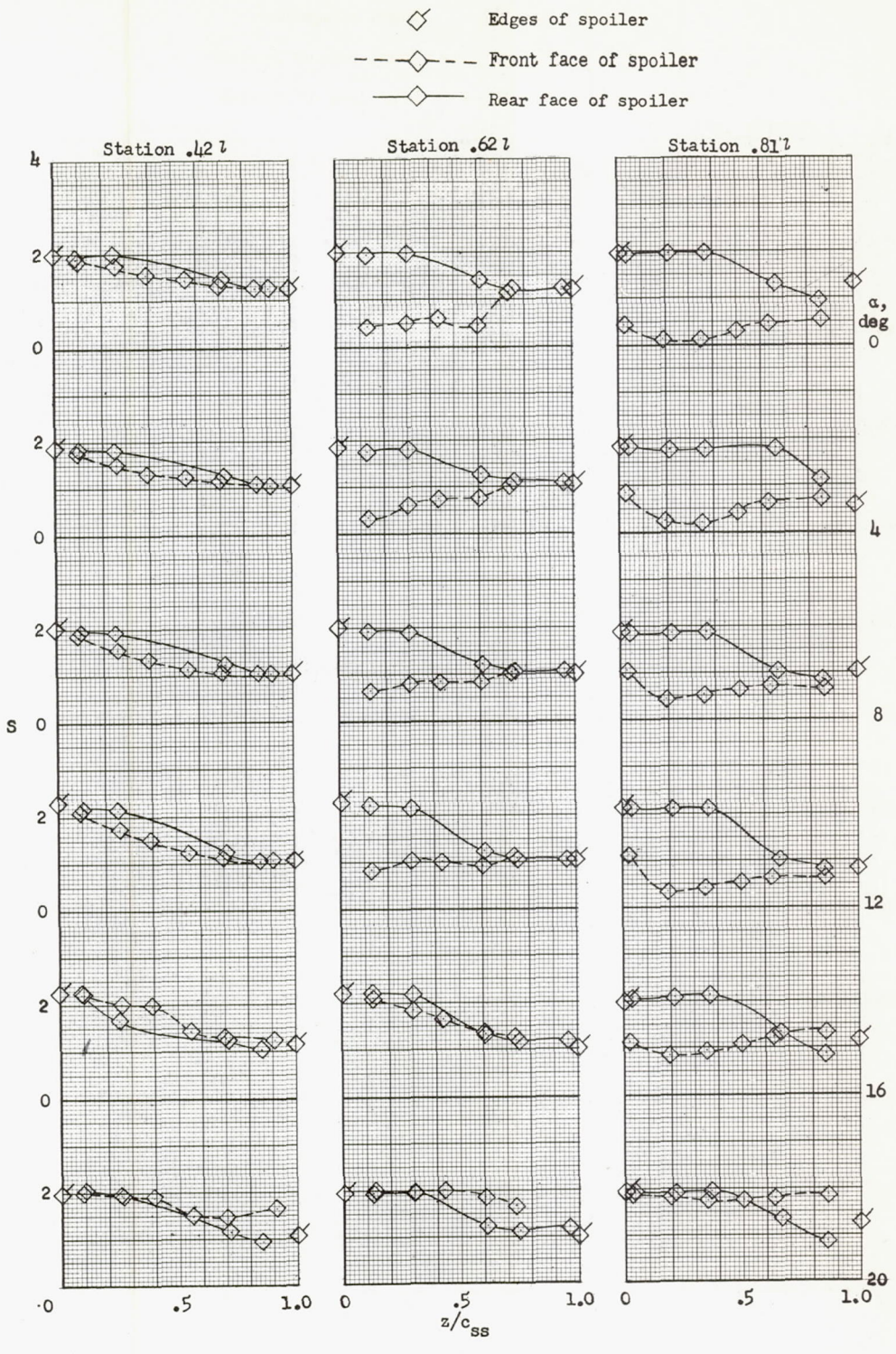

(g) M = 0.60; δ_{ss} = -30°.

Figure 4.- Continued.

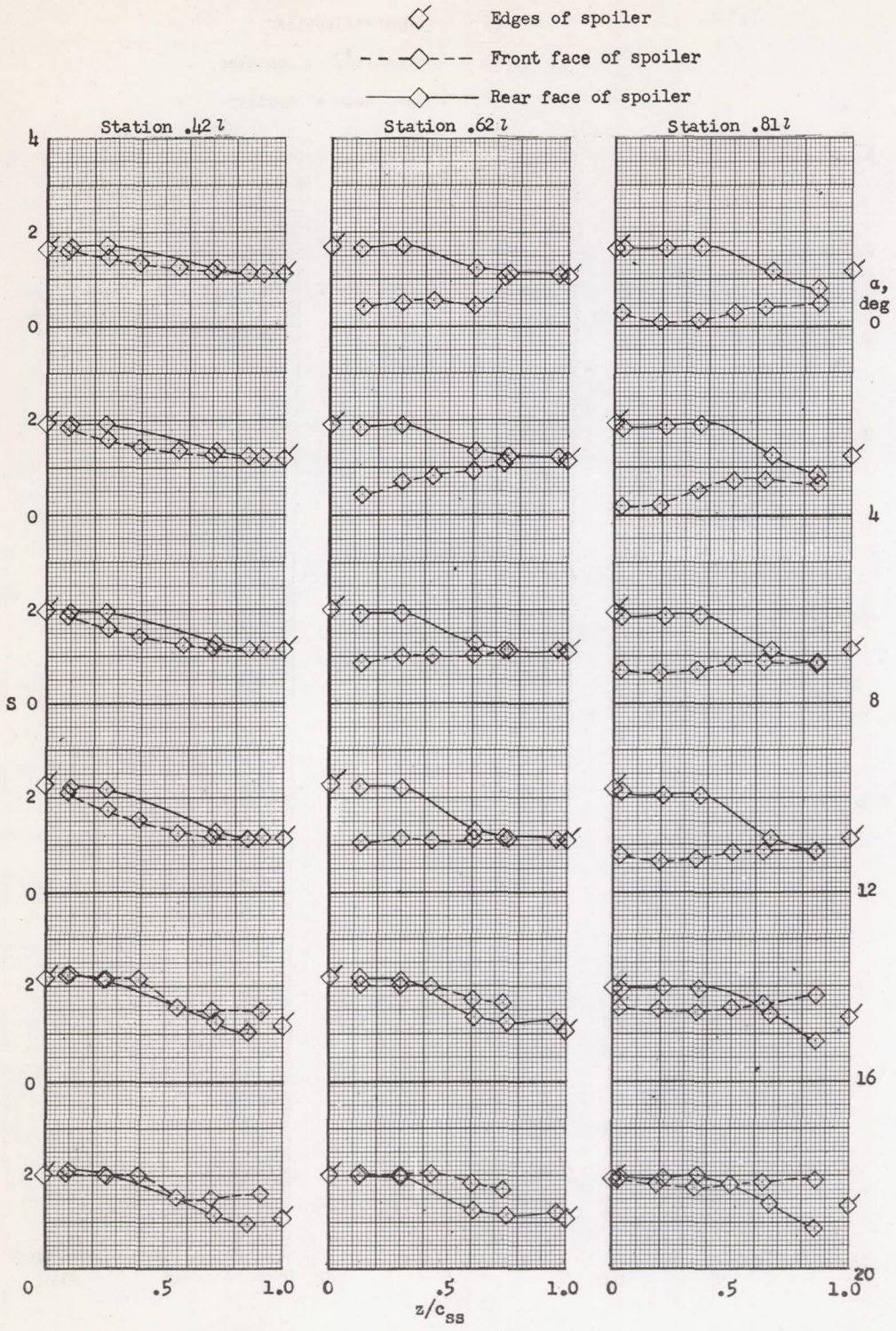

(h) $M = 0.80$; $\delta_{ss} = -30^{\circ}$.

Figure 4.- Continued.

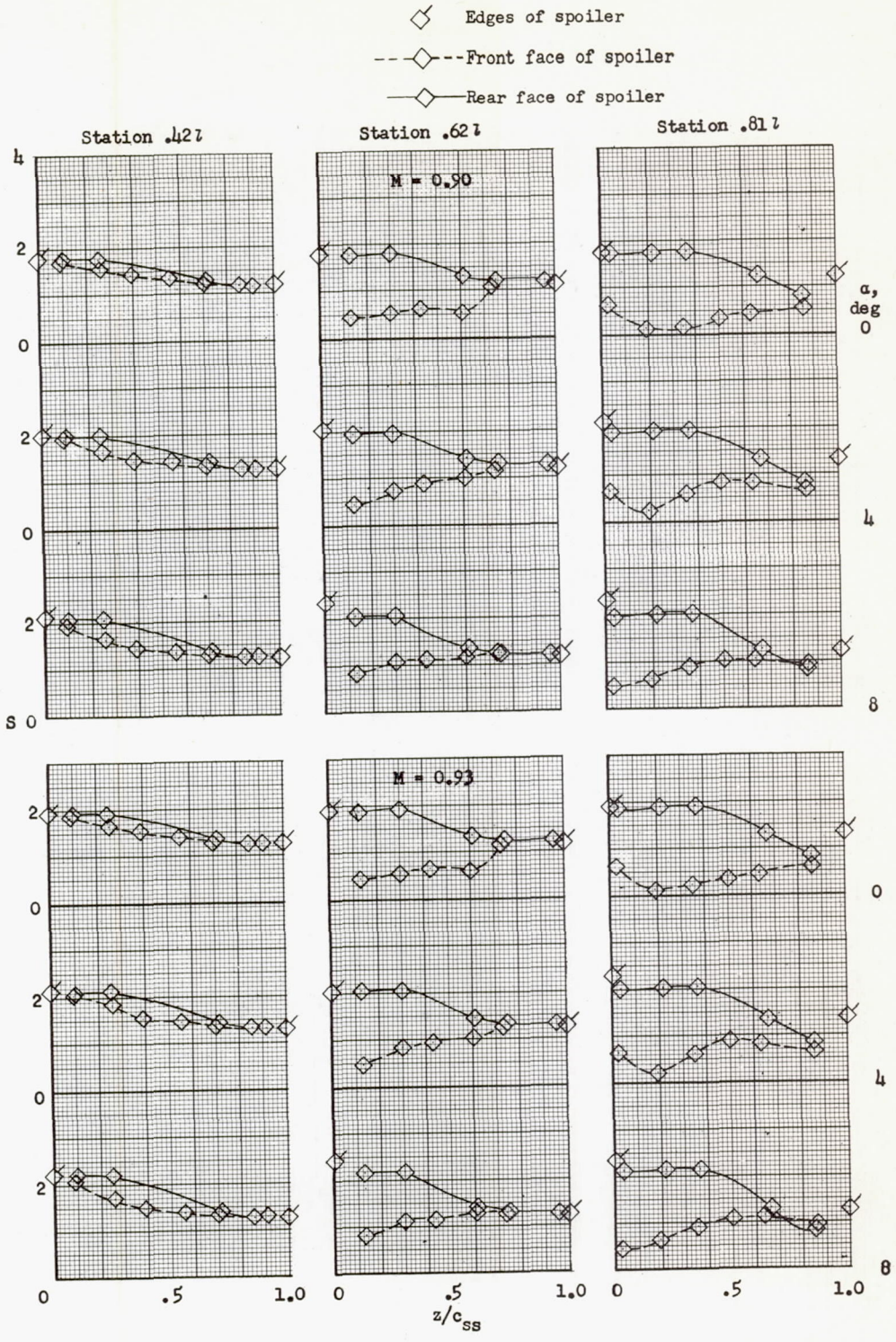

(i) M = 0.90, 0.93; $\delta_{SS} = -30^{\circ}$.

Figure 4.- Continued.

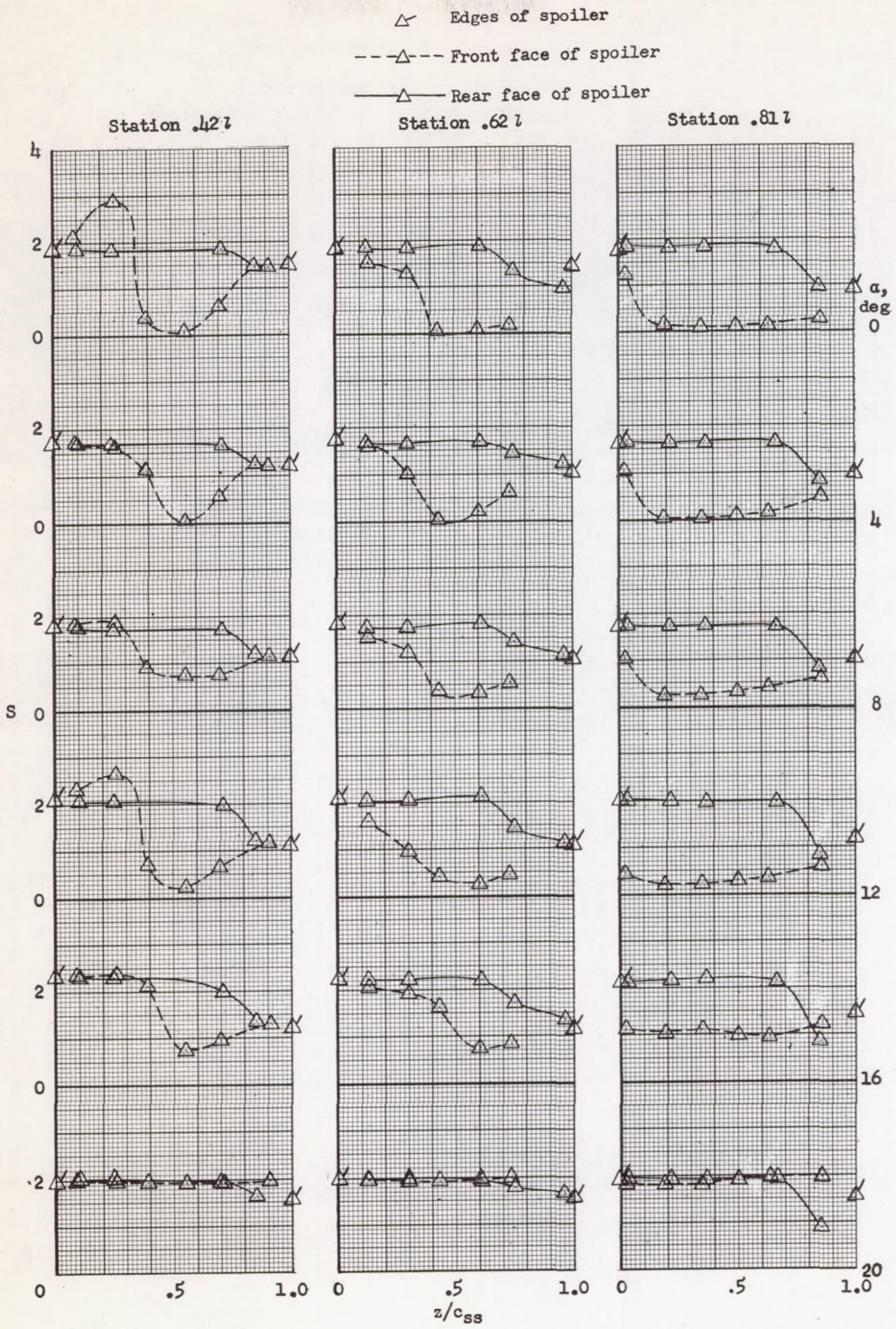

(j) M = 0.60; δ_{ss} = -45°.

Figure 4.- Continued.

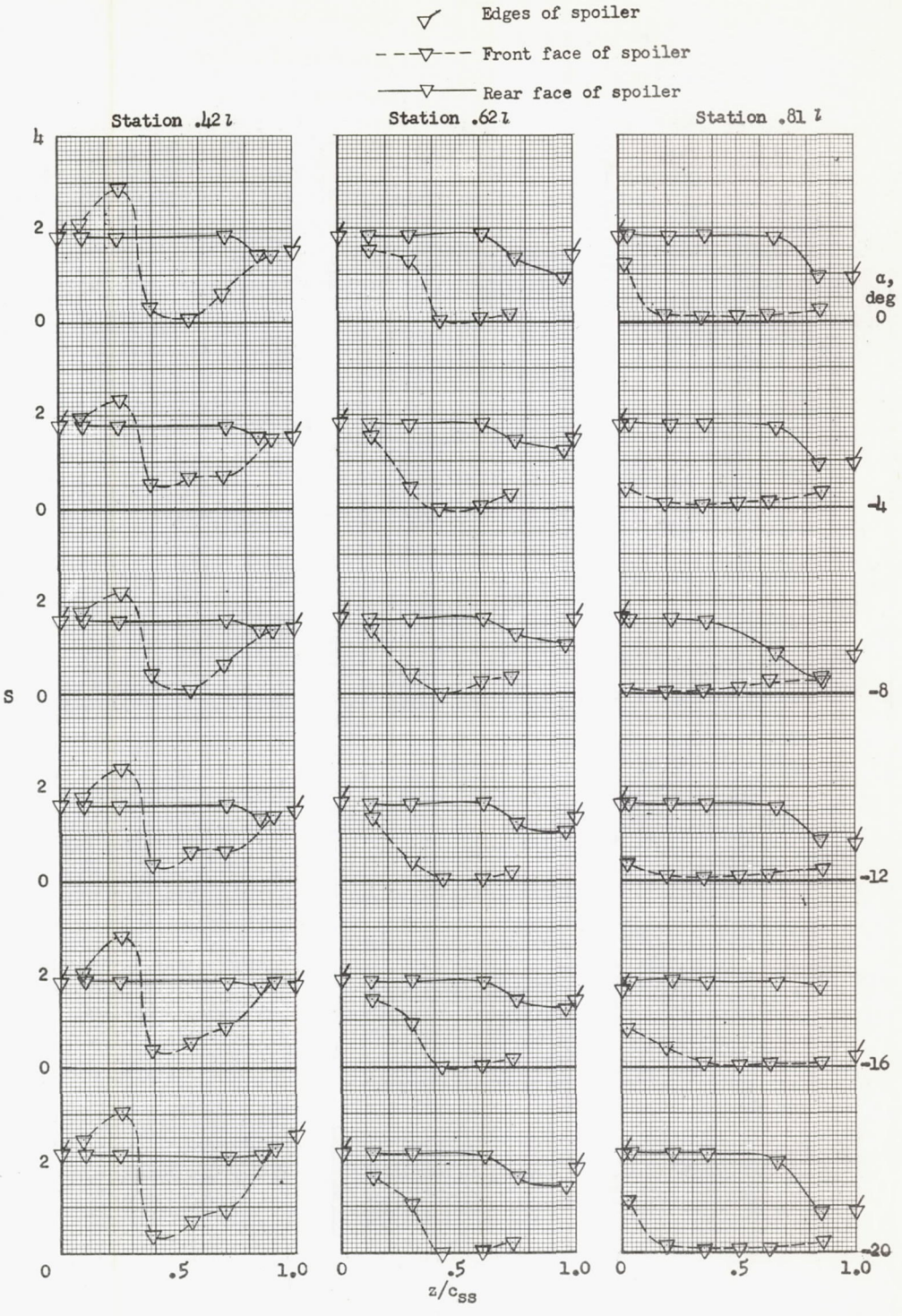

(j) Concluded.

Figure 4.- Continued.

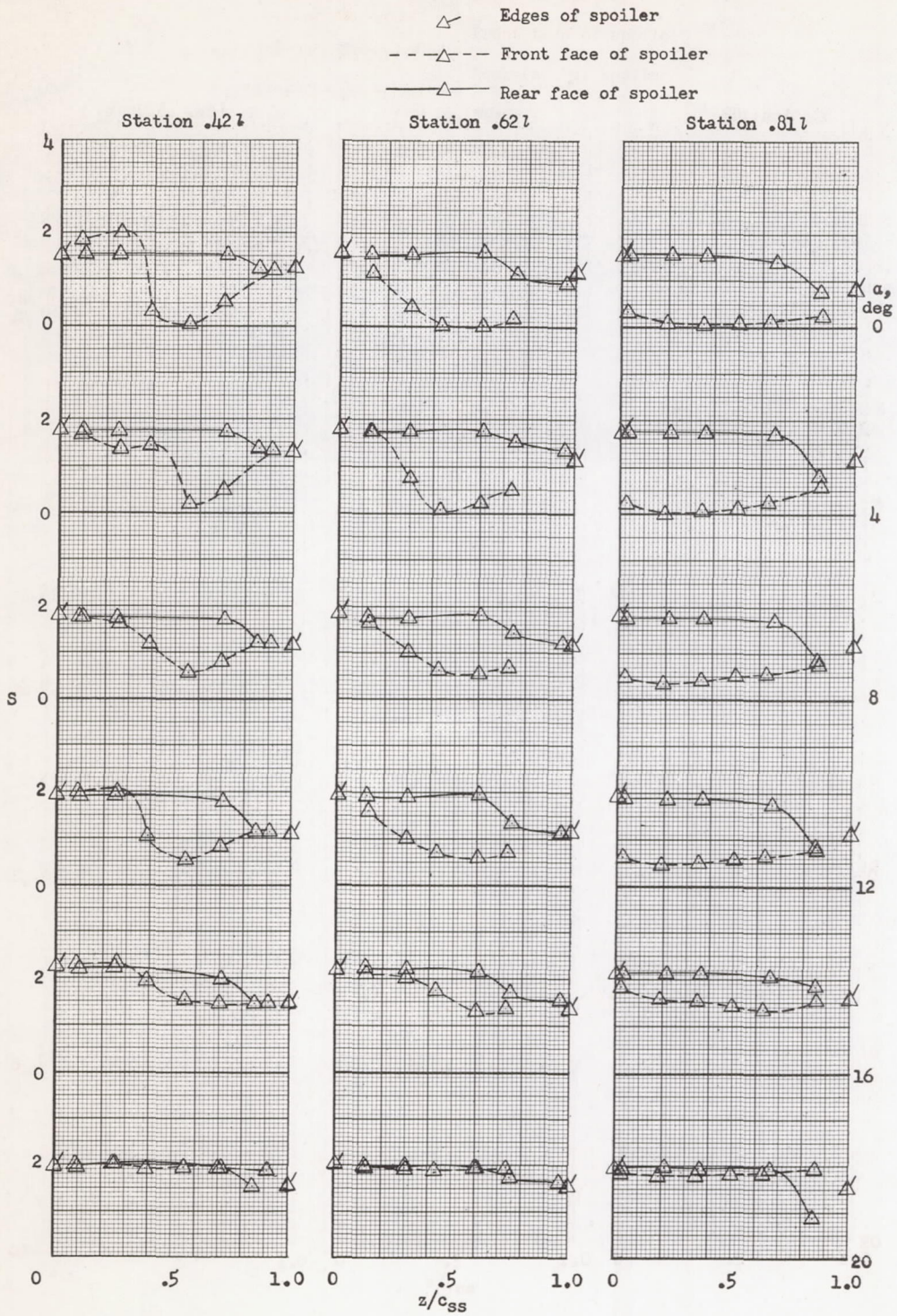

(k) M = 0.80; δ_{ss} = -45°.

Figure 4.- Continued.

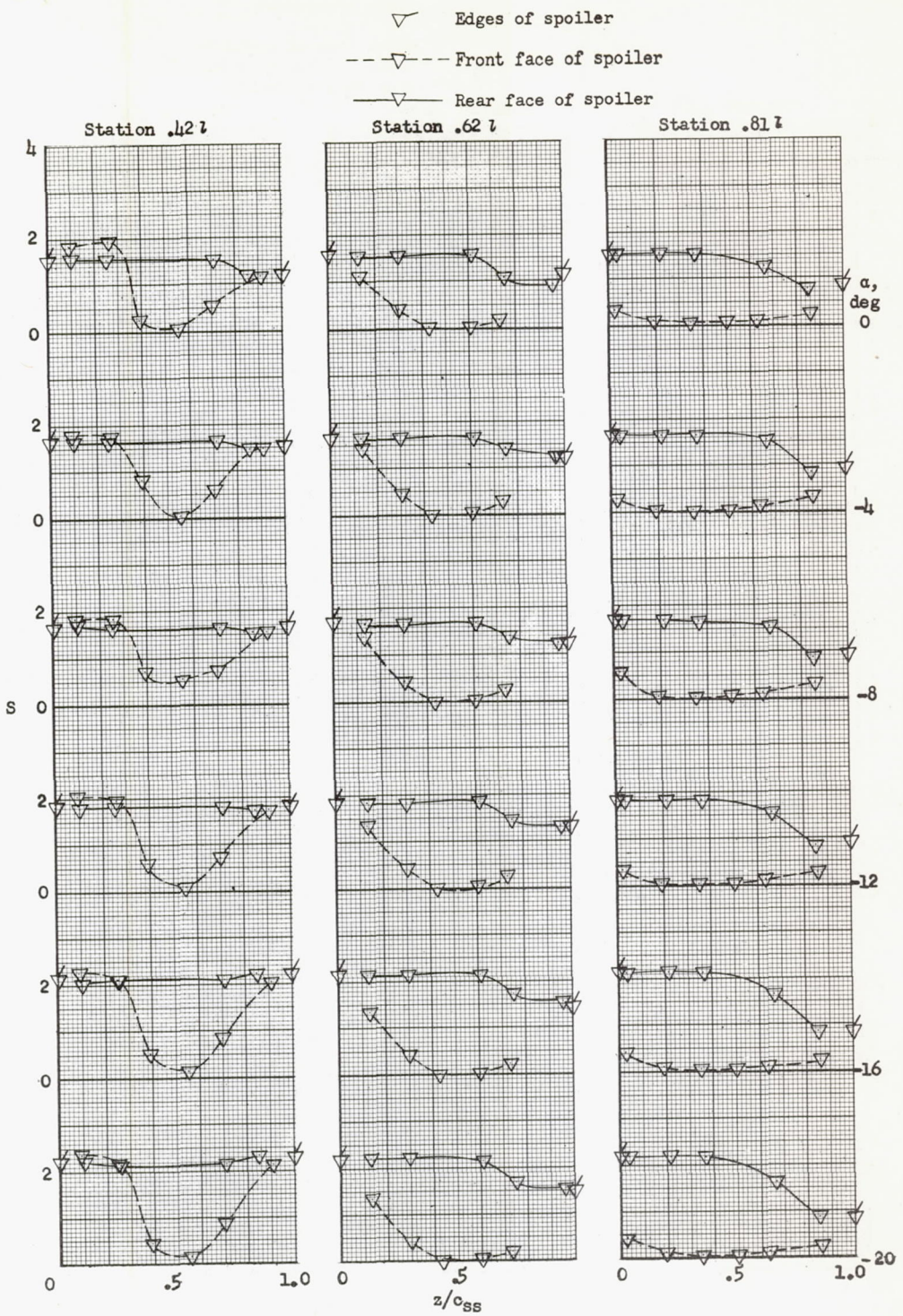

(k) Concluded.

Figure 4.- Continued.

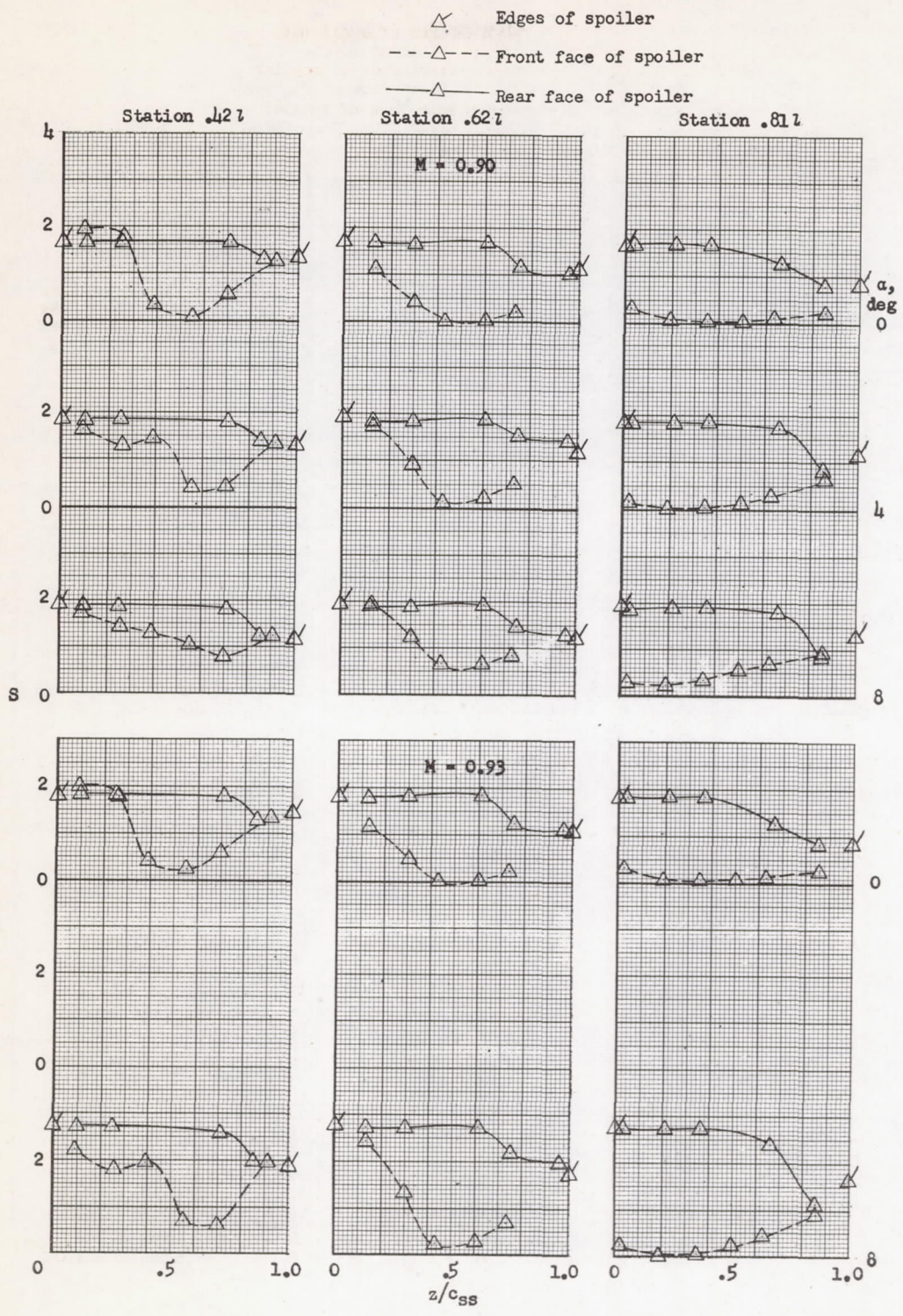

(l) M = 0.90, 0.93; δ_{ss} = -45°./

Figure 4.- Continued.

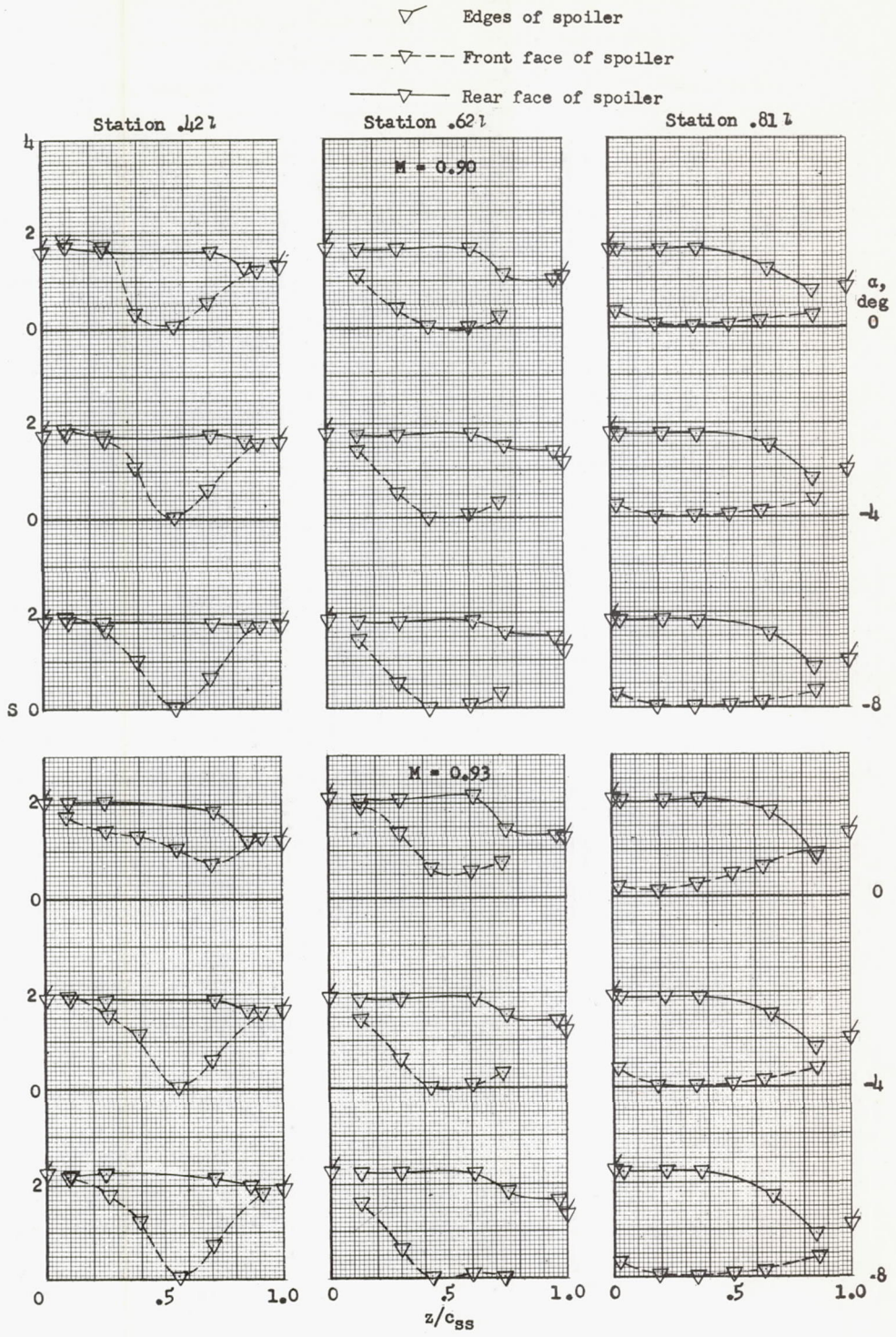

(l) Concluded.

Figure 4.- Concluded.

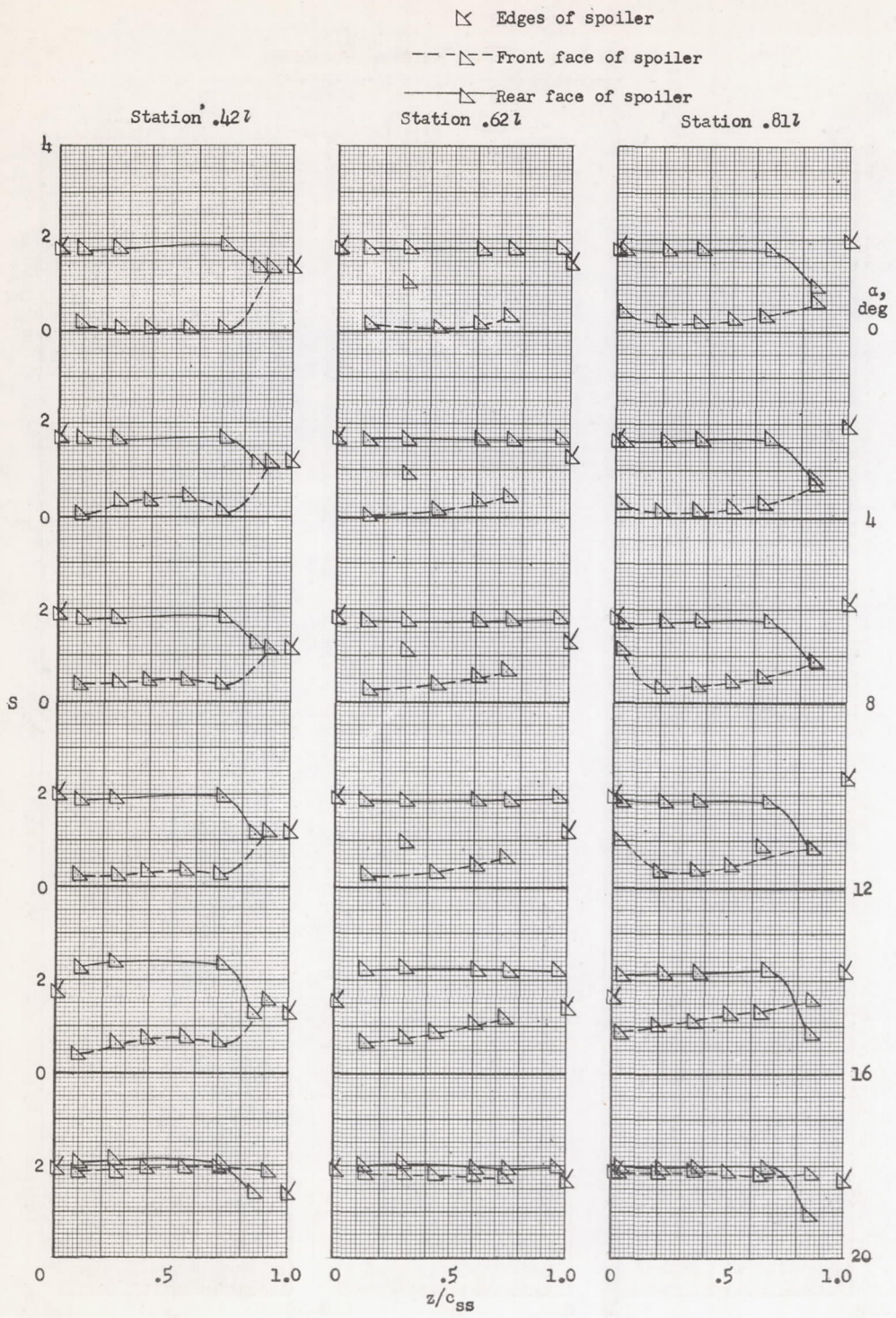

(a) $M = 0.60$; $\delta_{ss} = -45^{\circ}$.

Figure 5.- Pressure coefficient on a semaphore spoiler at three stations on the spoiler. Single semaphore spoiler deflected.

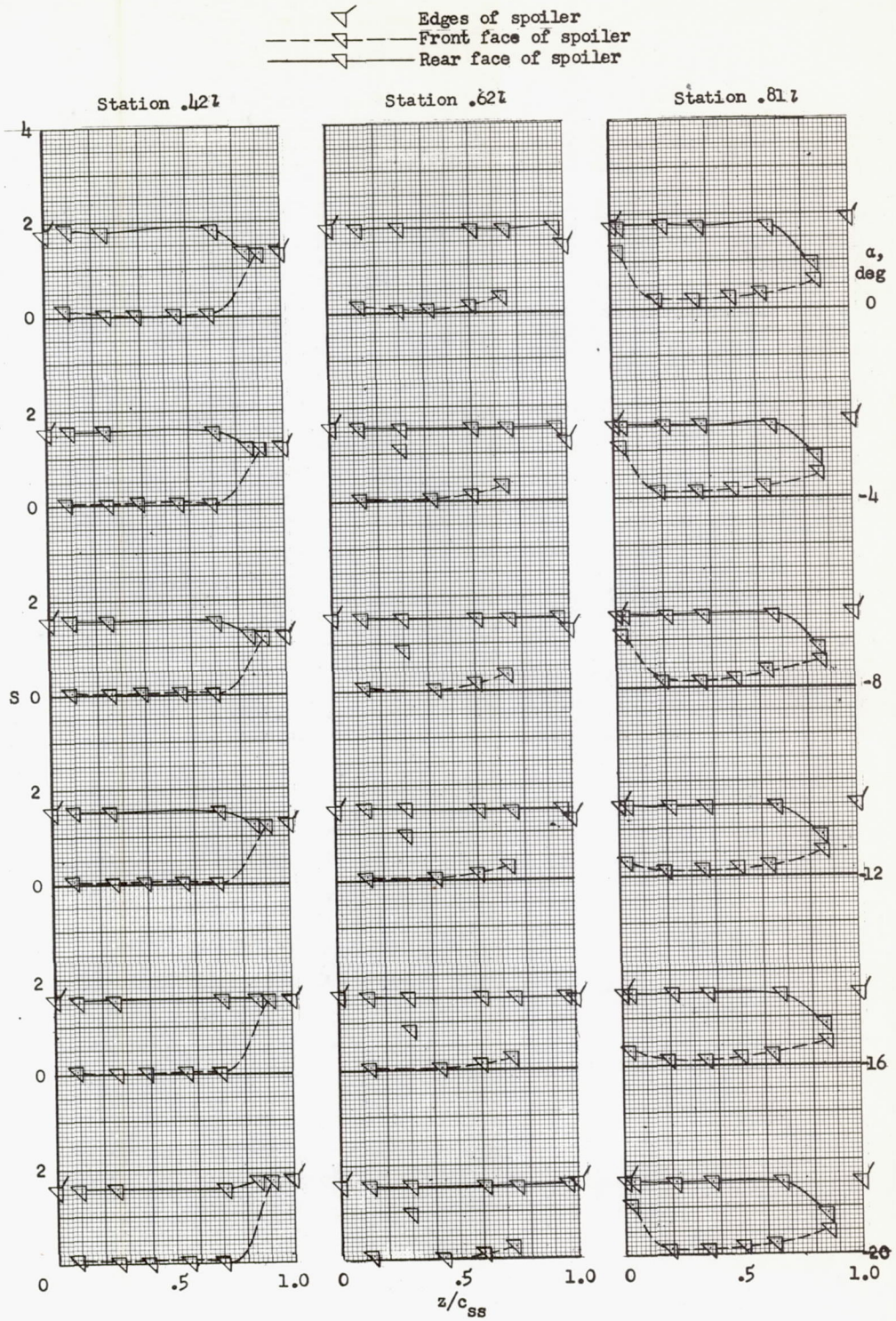

(a) Concluded.

Figure 5.- Continued.

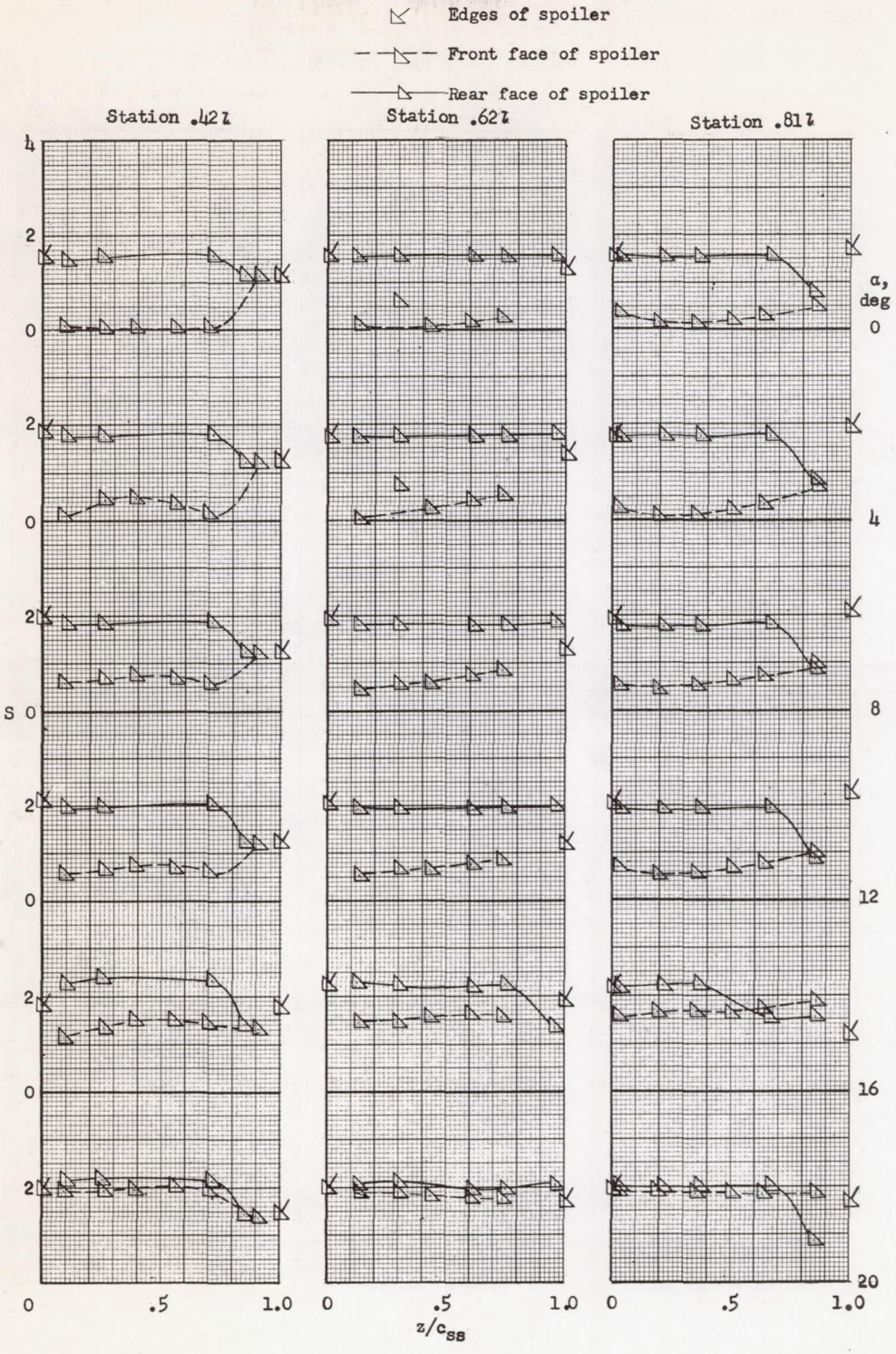

(b) M = 0.80; δ_{ss} = -45°.

Figure 5.- Continued.

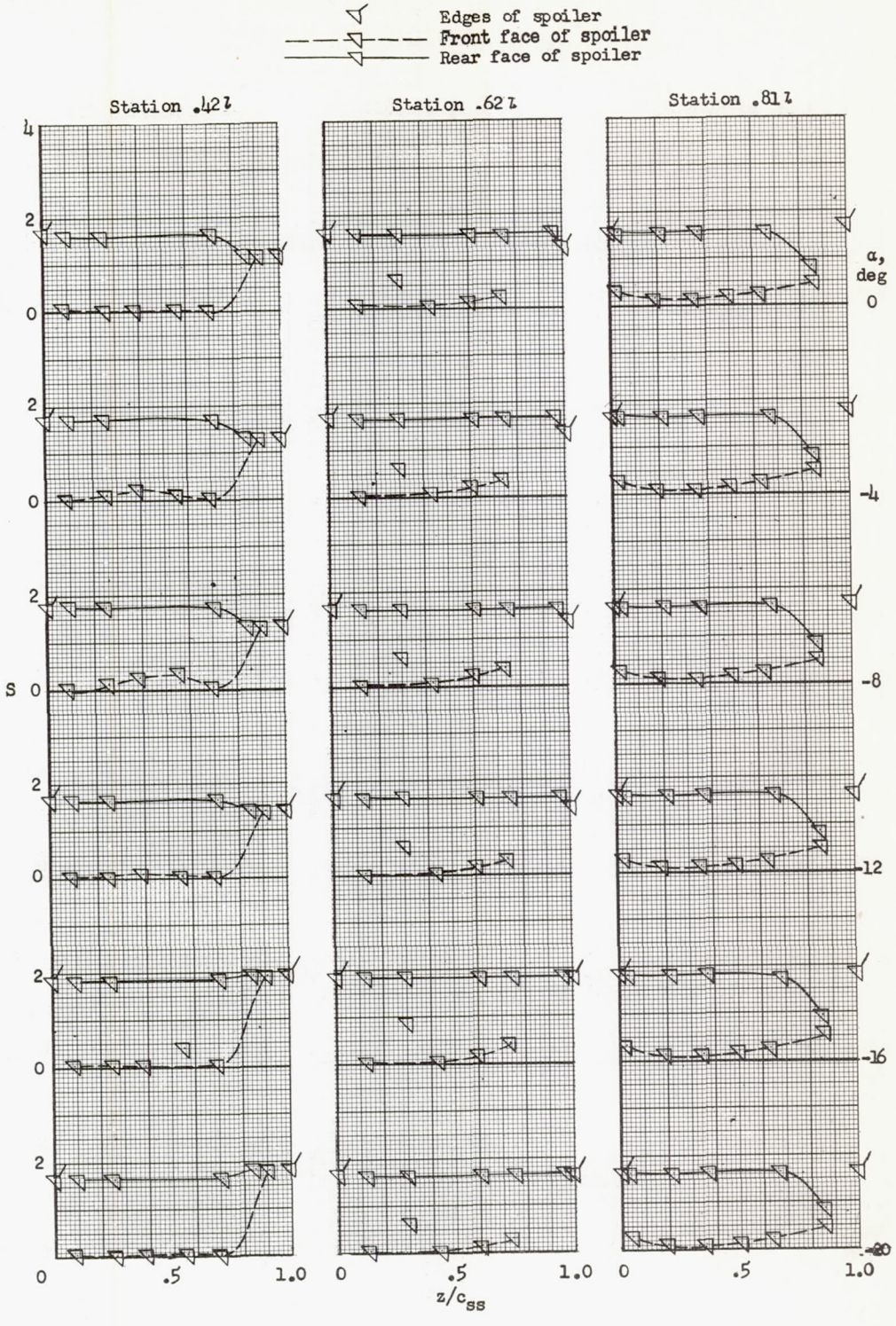

(b) Concluded.

Figure 5.- Continued.

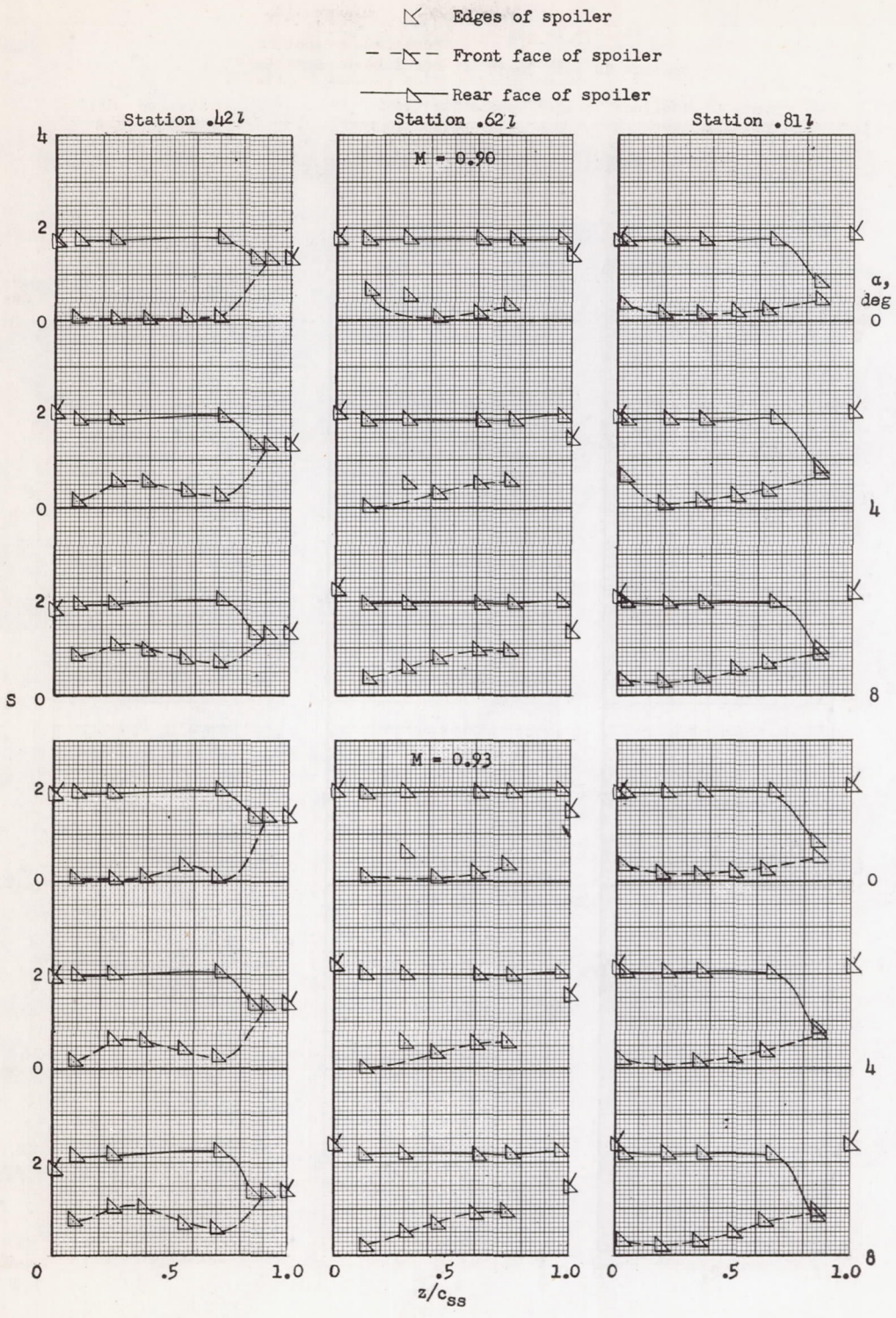

(c) M = 0.90, 0.93; $\delta_{ss} = -45°$.

Figure 5.- Continued.

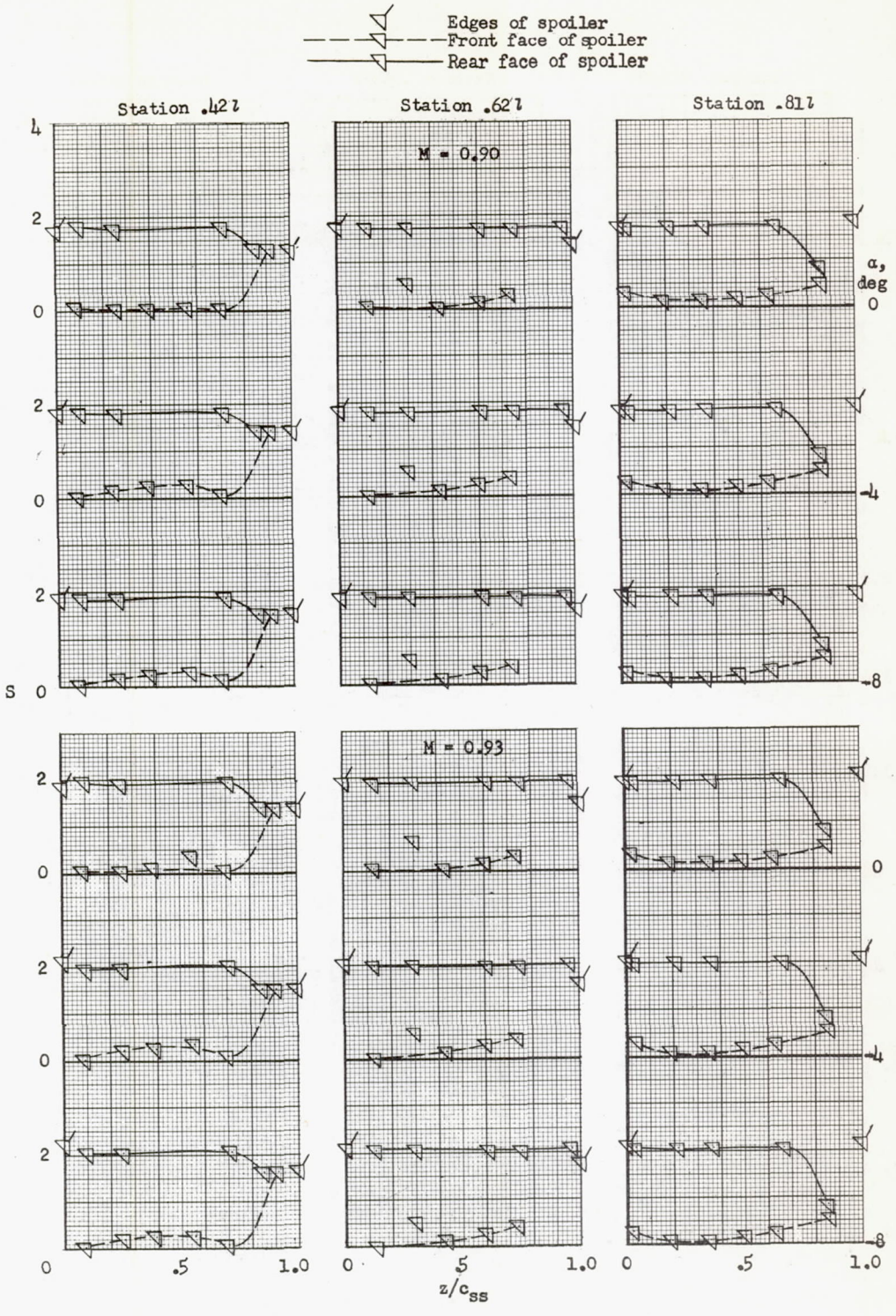

(c) Concluded.

Figure 5.- Concluded.

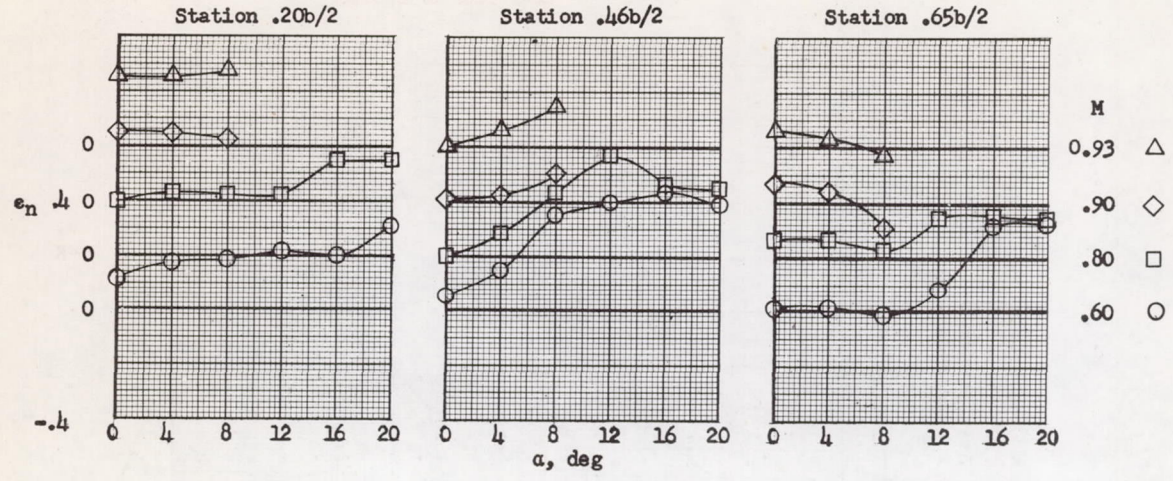

(a) $\delta_{ps} = 0.$

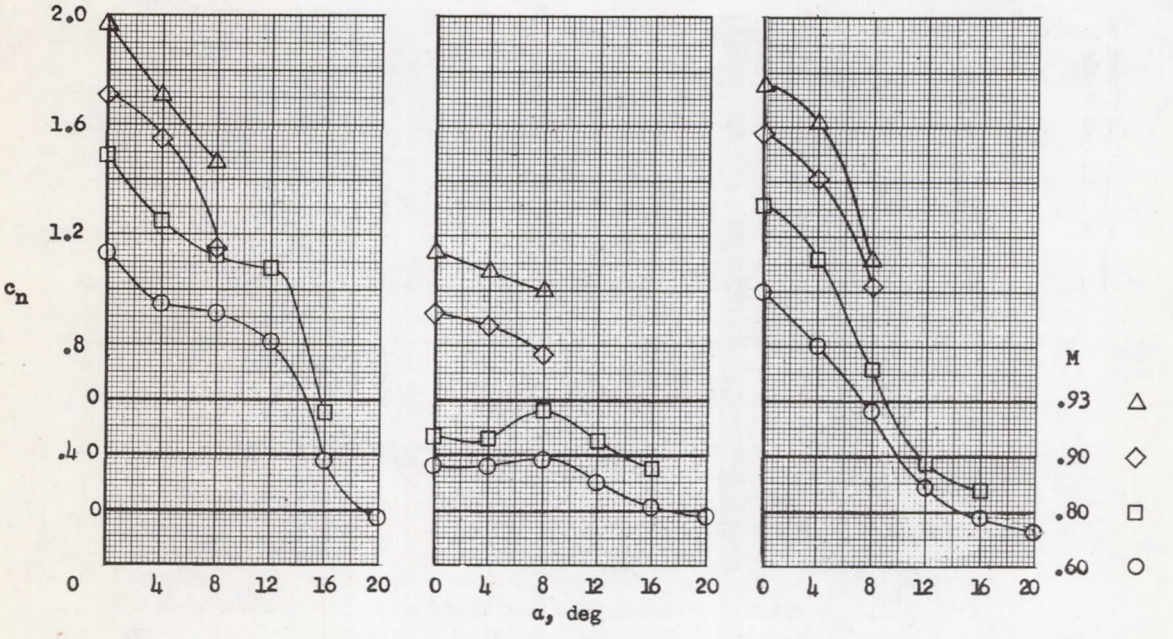

(b) $\delta_{ps} = -0.02c.$

Figure 6.- Variation of section normal force coefficient on plug spoiler with angle of attack for several Mach numbers at three spanwise stations. Coefficients are mathematically integrated by the rectangular-step method.

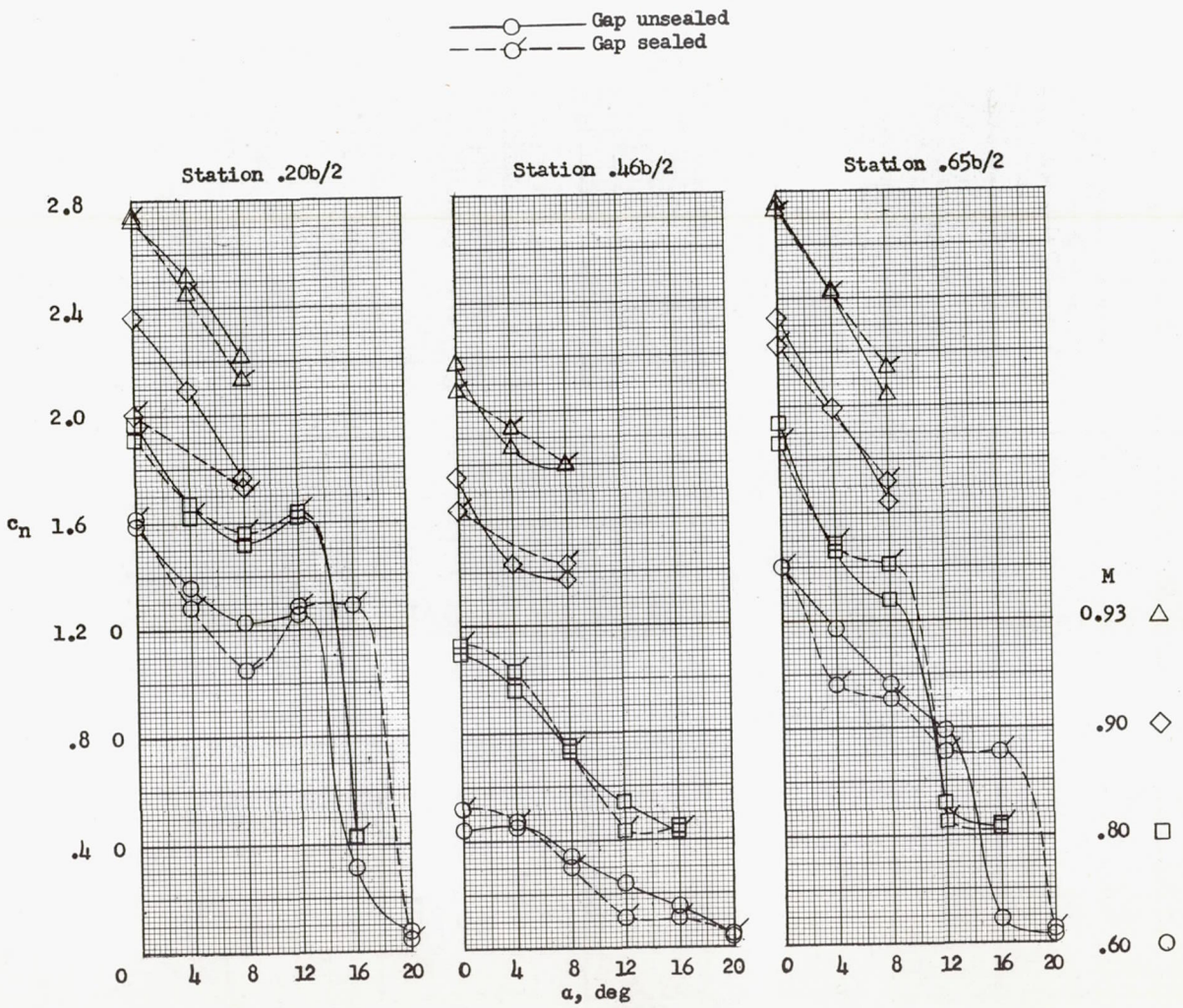

(c) $\delta_{ps} = -0.04c$.

Figure 6.- Concluded.

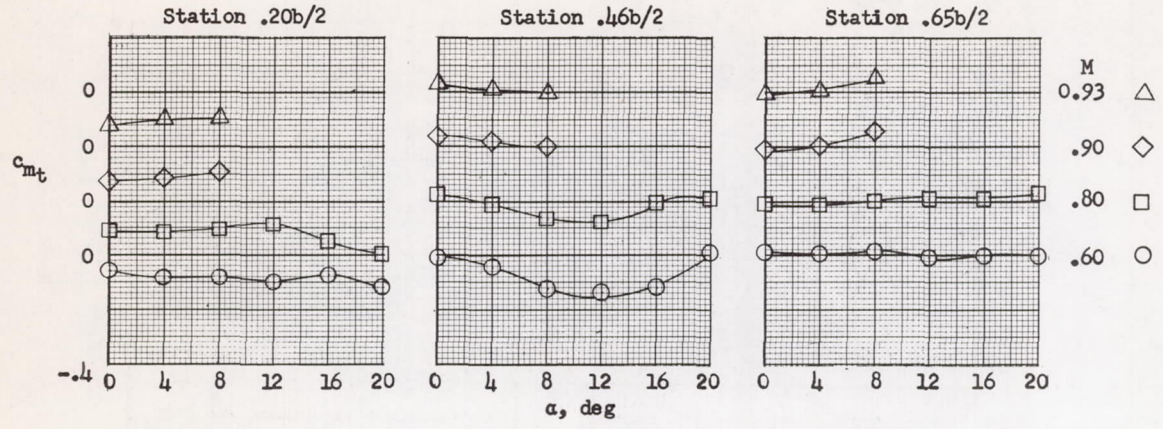

(a) $\delta_{ps} = 0.$

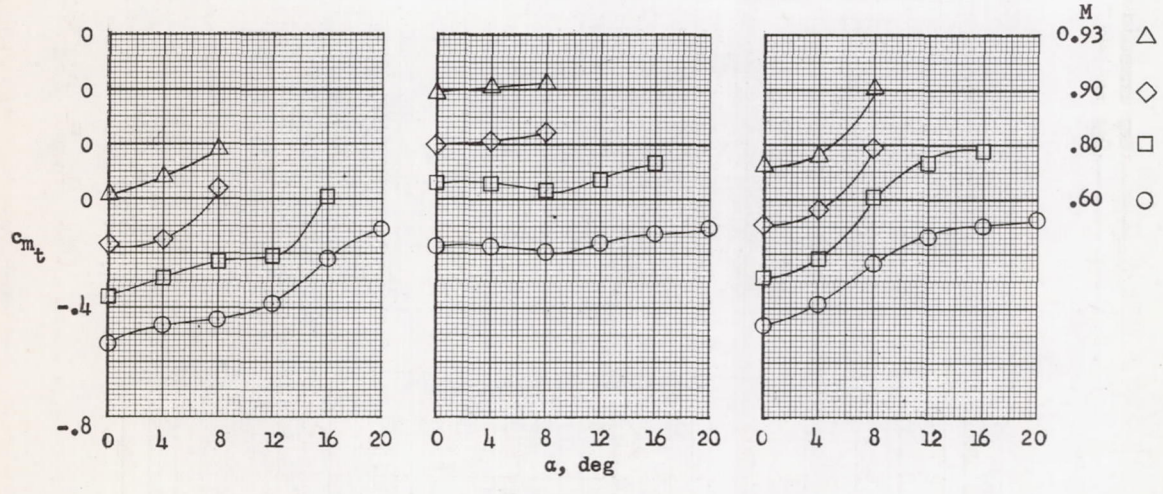

(b) $\delta_{ps} = -0.02c.$

Figure 7.- Variation of section twisting-moment coefficient with angle of attack for several Mach numbers at three spanwise stations on the plug spoiler. Coefficients are mathematically integrated by the rectangular-step method.

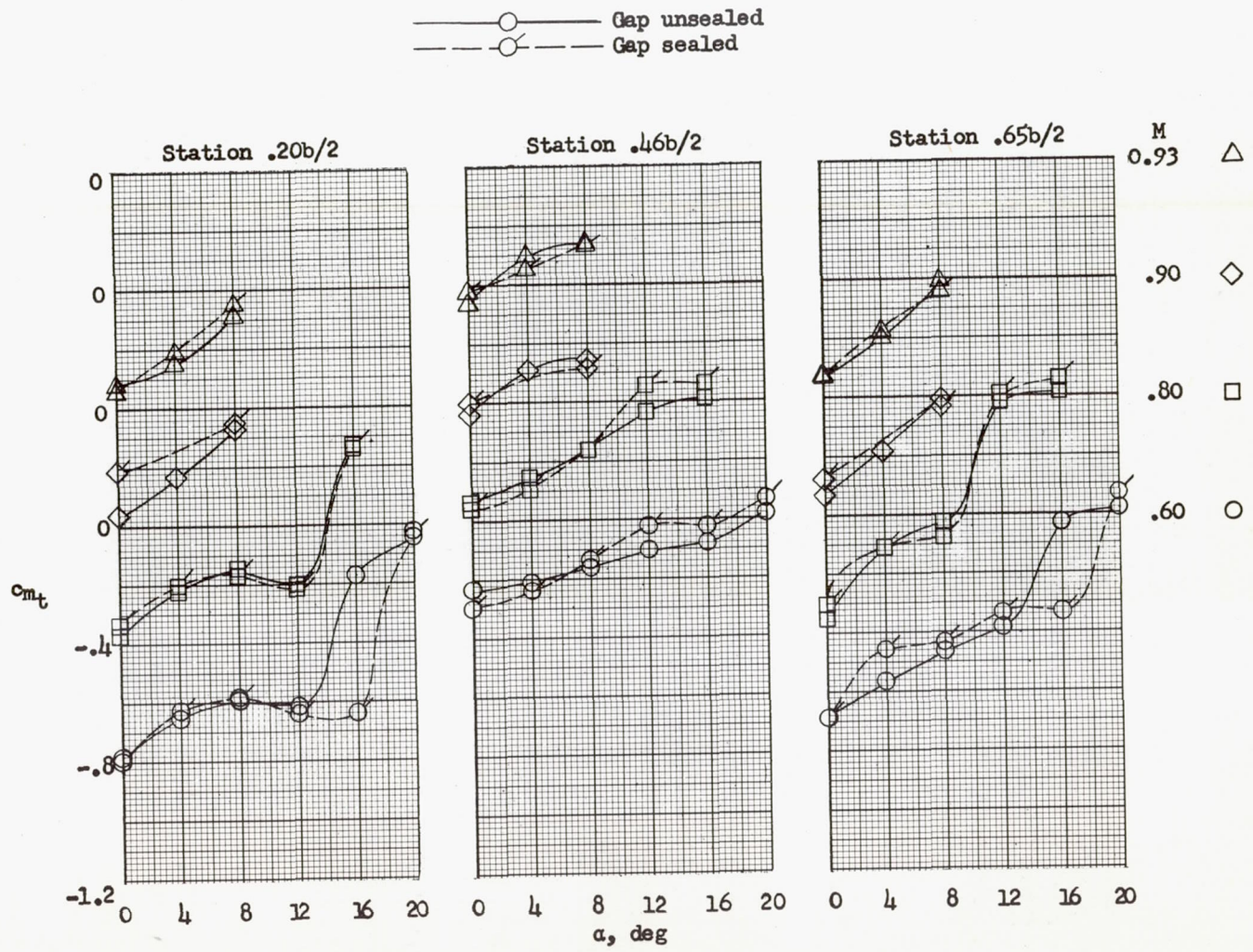

(c) $\delta_{ps} = -0.04c$.

Figure 7.- Concluded.

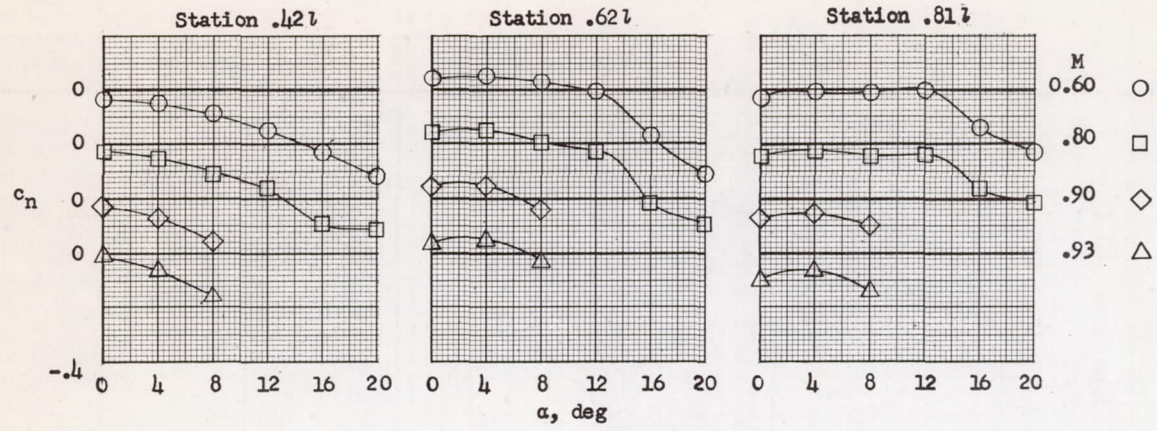

(a) $\delta_{ss} = 0.$

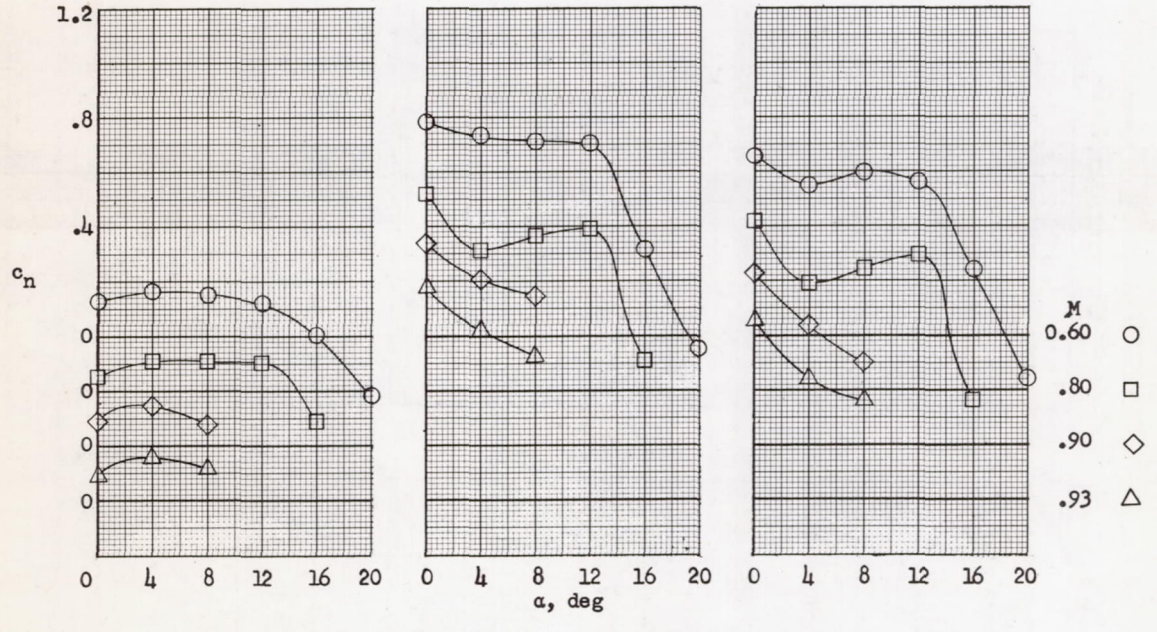

(b) $\delta_{ss} = -15^{\circ}.$

Figure 8.- Variation of section normal-force coefficient with angle of attack for several Mach numbers at three stations on the semaphore spoiler. Coefficients are mathematically integrated by the rectangular-step method. All spoilers were at same deflection angle except figure 8(c) where single spoiler deflected.

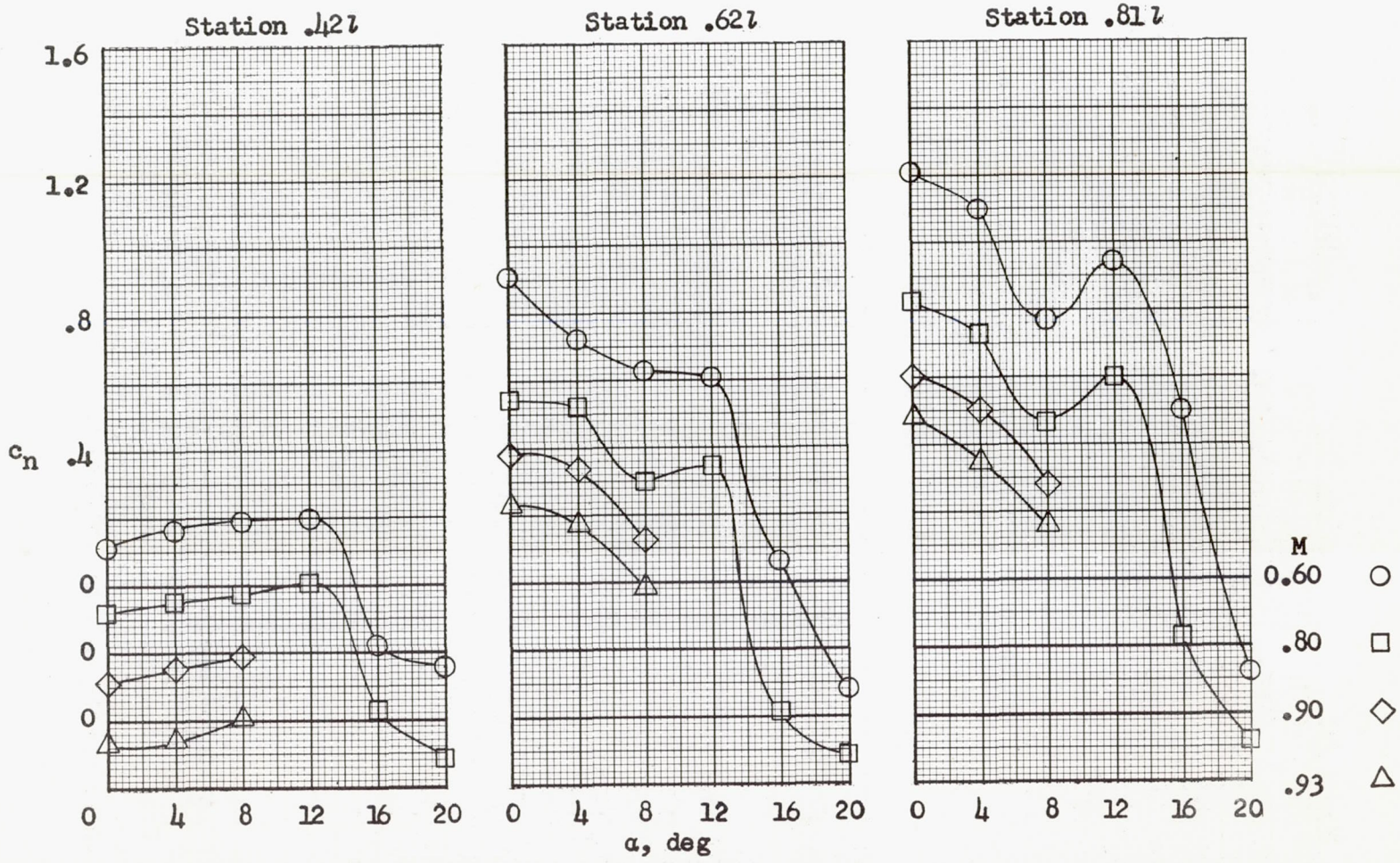

(c) $\delta_{ss} = -30^{\circ}$.

Figure 8.- Continued.

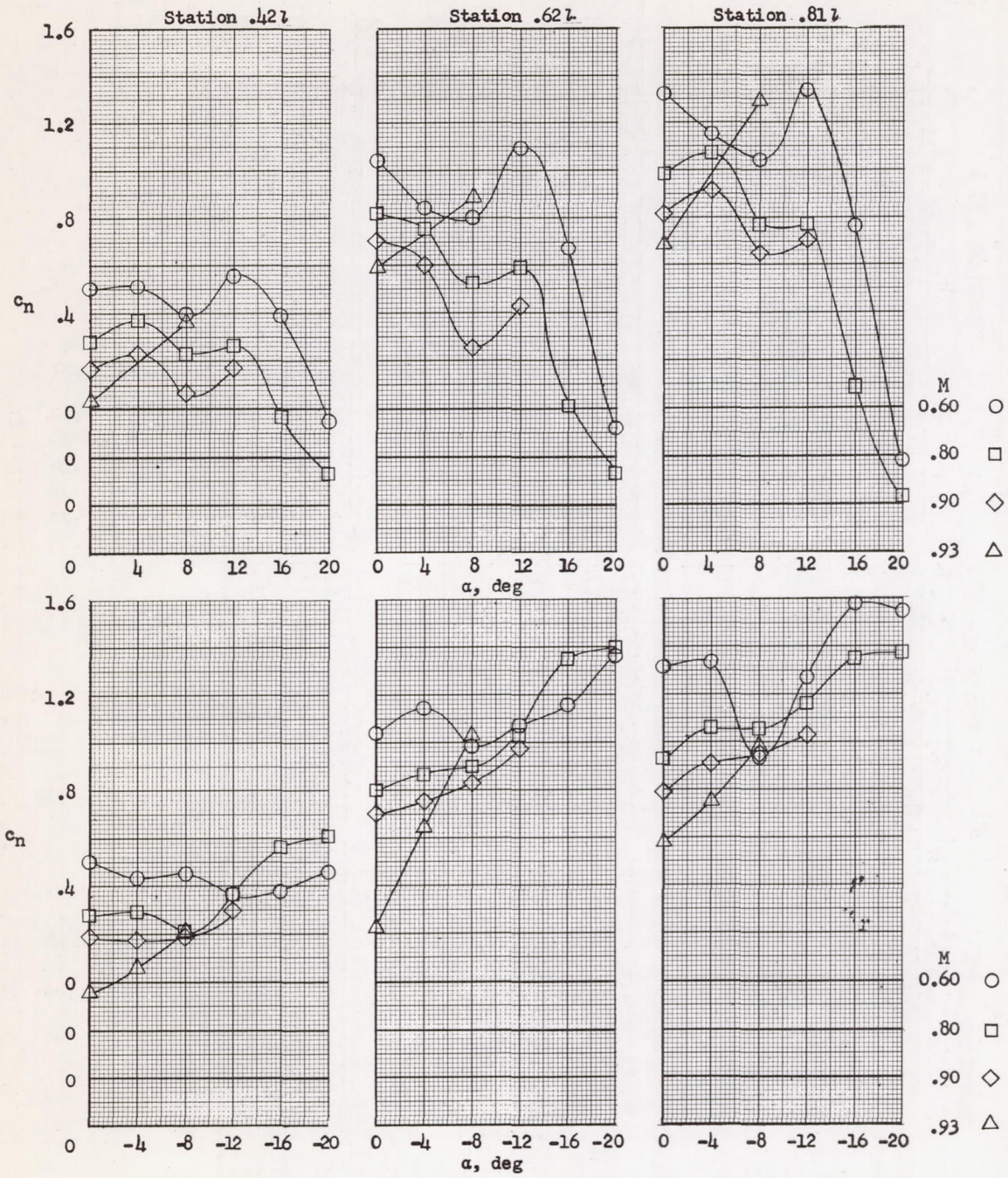

(d) $\delta_{ss} = -45°$.

Figure 8.- Continued.

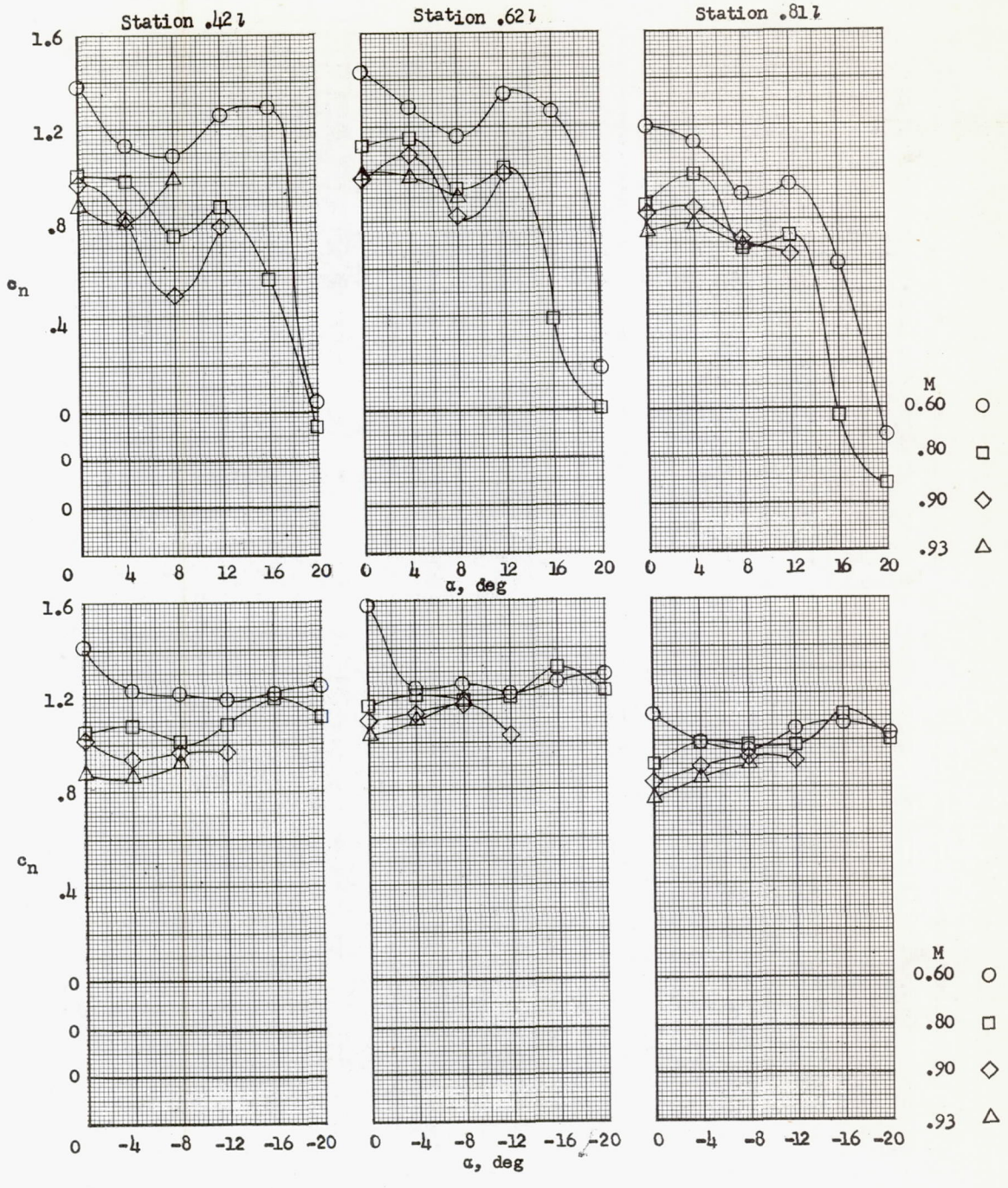

(e) $\delta_{ss} = -45^{\circ}$.

Figure 8.- Concluded.

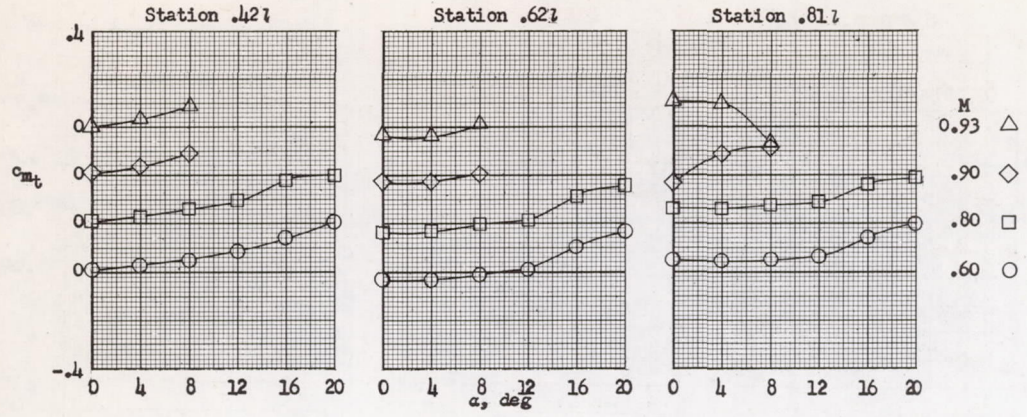

(a) $\delta_{ss} = 0.$

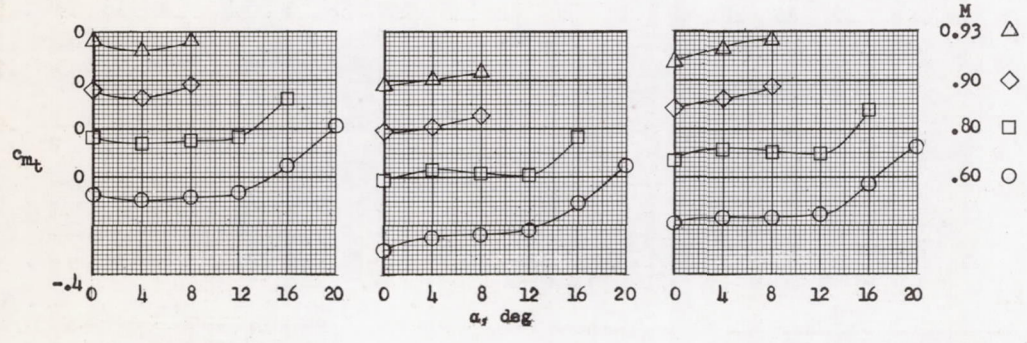

(b) $\delta_{ss} = -15^{\circ}.$

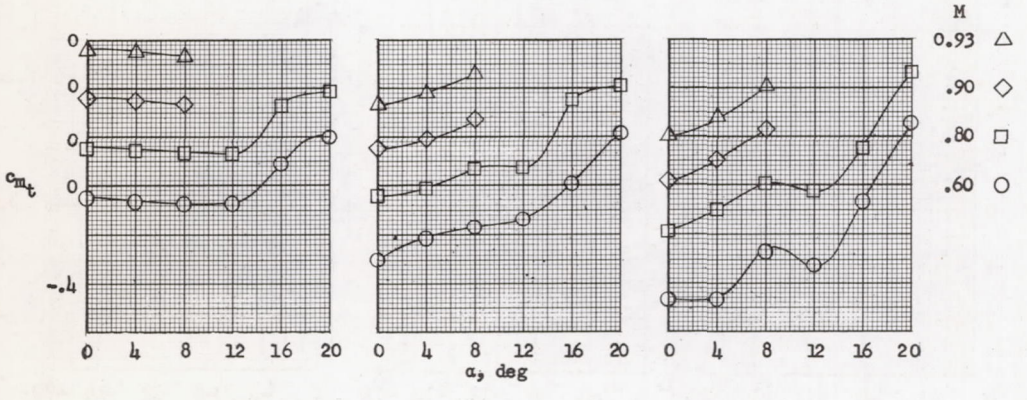

(c) $\delta_{ss} = -30^{\circ}.$

Figure 9.- Variation of section twisting-moment coefficient with angle of attack for several Mach numbers at three stations on the semaphore spoiler. Coefficients are mathematically integrated by rectangular-step method. All spoilers deflected except for figure 9(e) where single spoiler deflected.

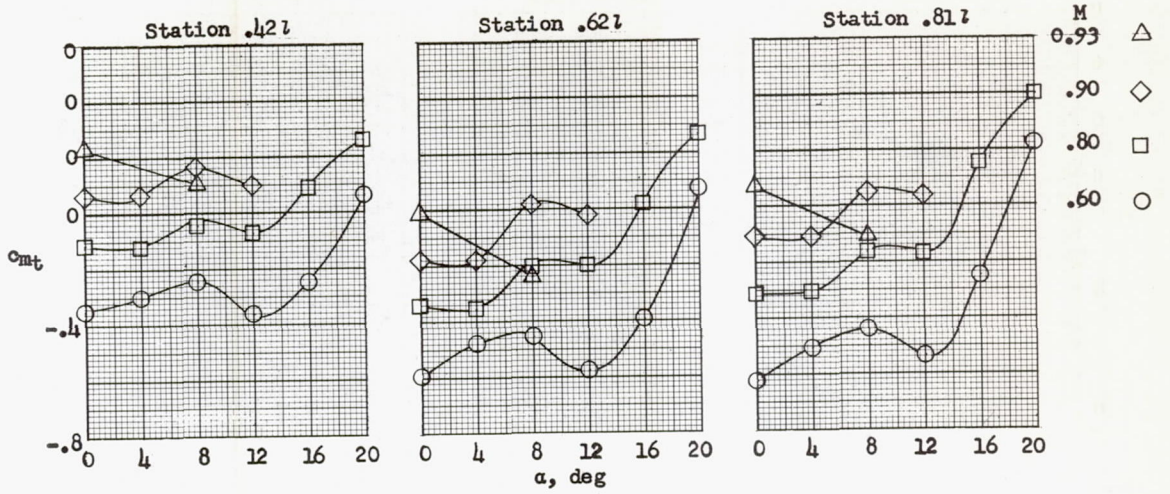

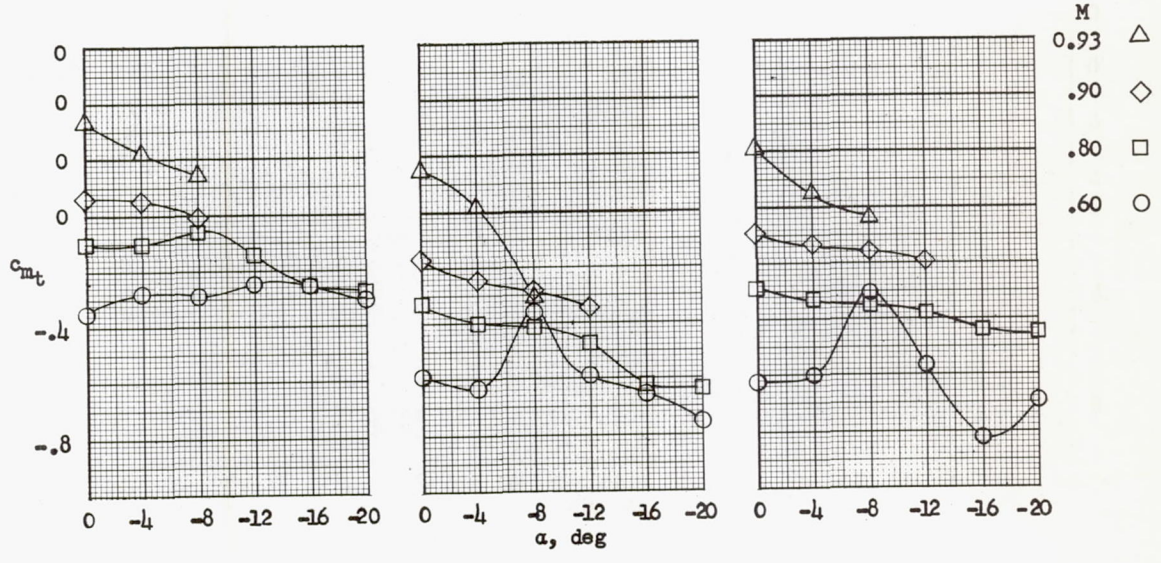

(d) $\delta_{ss} = -45^{\circ}$.

Figure 9.- Continued.

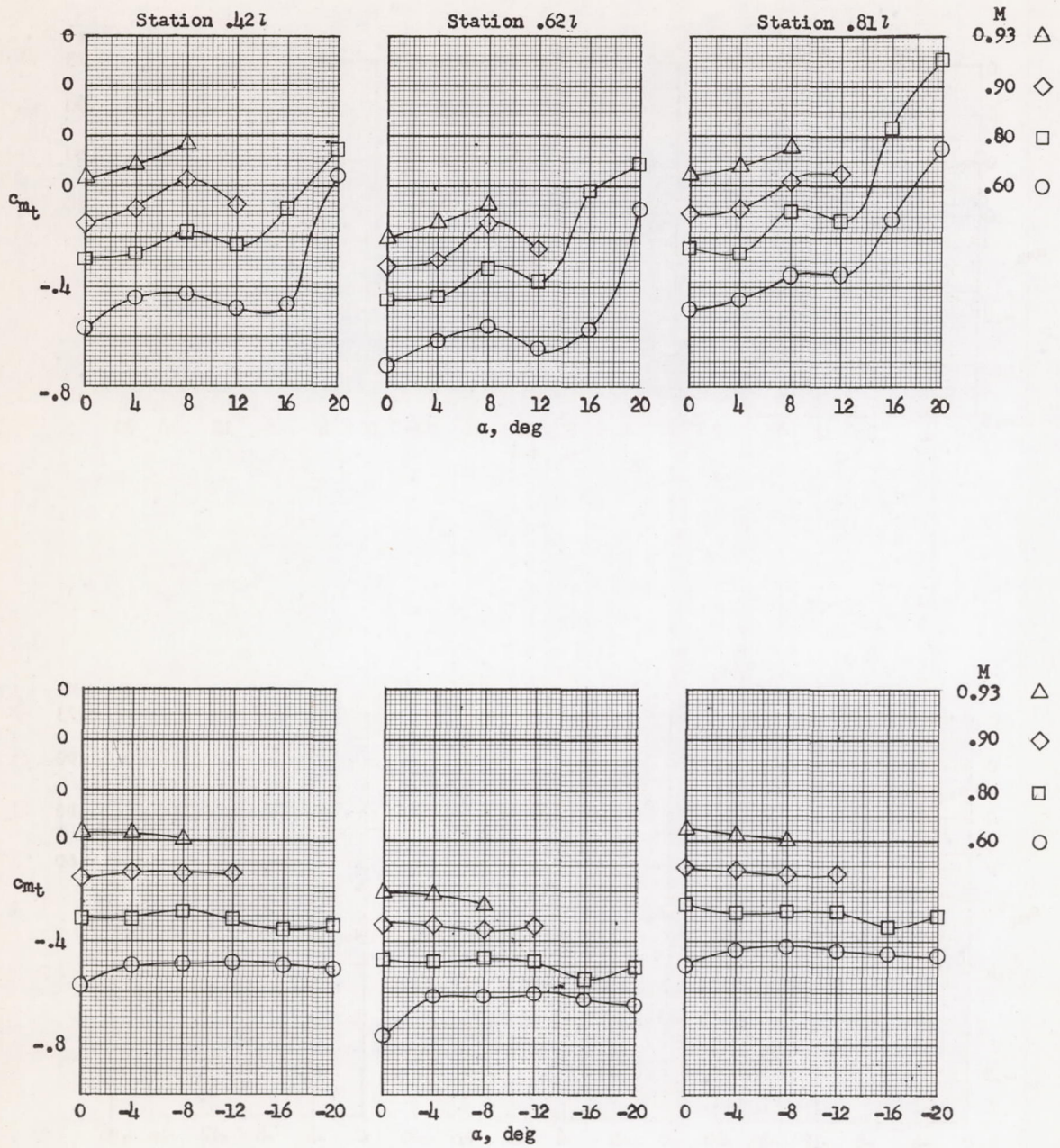

(e) $\delta_{ss} = -45^{\circ}$.

Figure 9.- Concluded.

NACA-Langley - 8-30-54 - 350